NASA Technical Memorandum 105658

Radial Turbine Cooling

Richard J. Roelke
Lewis Research Center
Cleveland, Ohio

Presented at the
Lecture Series on "Radial Turbines"
at the the von Karman Institute for Fluid Dynamics
Brussels, Belgium, April 6–10, 1992

NASA

RADIAL TURBINE COOLING

Richard J. Roelke
NASA Lewis Research Center
Cleveland, Ohio USA

INTRODUCTION

Radial turbines have been used extensively in many applications including small ground-based electrical power generators, automotive engine turbochargers and aircraft auxiliary power units. In all of these applications the turbine-inlet temperature is limited to a value commensurate with the material strength limitations and life requirements of uncooled metal rotors. To take advantage of the benefits that higher turbine-inlet temperatures offer, such as increased turbine specific power output or higher cycle thermal efficiency, requires improved high-temperature materials and/or blade cooling. Extensive research is on going to advance the material properties of high-temperature superalloys and composite materials, including ceramics. The use of ceramics with their high-temperature potential and low cost is particularly appealing for radial turbines. Japanese manufacturers have developed ceramic turbine technology to the point where it is being used in automotive turbochargers for their domestic market. A multiyear program is also underway in the United States to develop the ceramic material technology to enable an automotive gas-turbine engine to operate at a turbine-inlet temperature of 2500 °F (1370 °C). However, until these programs reach fruition, the only way to significantly increase operating temperatures in the face of present material temperature barriers is to cool the radial blading.

Turbine-blade cooling has been successfully accomplished for axial machines of all sizes. The cooling of radial turbines has not advanced at anywhere near the same rate. Perhaps, the main reason is the almost total use of axial turbines in high-technology aircraft engines. Initially, it would appear that cooling radial turbines would have distinct advantages over the cooling of axial turbines. The high-power output of a radial stage can replace two axial stages significantly reducing the number of parts that have to be cooled. Even on a per stage basis the radial turbine has fewer blades to cool. The high tip speed of a radial rotor also has the effect of reducing the relative gas temperature to which the rotor is subjected. These effects, higher work extraction per stage, lower relative temperature, and lower part count, have the potential of reducing the amount of coolant required for the radial turbine as compared with the axial turbine for the same inlet temperature. Also, where the radial turbine offers an attractive alternate to the axial turbine, i.e., small turbines, the radial turbine has been shown to have a performance advantage. This should provide an impetus to increase the radial turbine operating temperature to further it's use. However, the cooling of a radial turbine has provided a significant challenge.

The challenges of cooling a radial turbine can be grouped into three areas: (1) minimizing the aerodynamic performance degradation caused by cooling constraints, (2) improving the analytical design procedures used to reach a viable design, and (3) developing fabrication technology that results in quality parts that meet life requirements and that are cost effective. The addition of blade cooling to a radial-turbine rotor can result in a lower tip speed, increased trailing-edge thickness, lower rotor reaction, and fewer rotor blades than would be selected if the rotor were uncooled. Each of these compromises can, if not treated carefully, lower the aerodynamic performance. Analytical prediction methods are necessary to estimate the hot-side local heat loads; coolant flow distribution, pressure loss, and heat addition; mechanical and thermal stresses; and component life. This is not any different from that required to design cooled axial turbine blades. However, the many successful cooled axial turbine designs have contributed to a vast database of what works and what does not. The different radial-rotor geometry with its highly three-dimensional flow field and, more particularly, the different manufacturing methods used, make use of this existing database difficult. The technology required to efficiently cool and fabricate the inlet vanes, however, is fairly well established and draws heavily from axial turbine experience. Cooling the flow path sidewalls (i.e. backface and shroud) presents new design problems but these are not perceived as major obstacles. This leaves the fabrication of a cooled rotor that meets material strength requirements and cost goals as a major hurdle to obtaining a satisfactory cooled radial turbine.

Typically, radial rotors are either integrally cast or machined from a forging. Fabricating the cooled rotor from an integral casting requires the use of multiple ceramic cores. The cores are long and thin and need to be supported adequately during the pouring process to avoid core shifting and wall breakout. The scrap rate would be expected to be high since a single bad blade in an otherwise good rotor makes the rotor unusable and therefore scrap. The magnitude of this problem is best illustrated by the following example. If the probability of casting an acceptable blade is 0.9 and the rotor contains 10 blades, the probability of having an acceptable rotor is $(0.9)^{10}=0.35$. Two-thirds of the cast rotors would be scrapped!

Conversely, starting with a forging is not particularly attractive. Drilling cooling holes in a forging would clearly be both time consuming and expensive and still may not create the internal geometry necessary for high cooling effectiveness. Clearly, formidable fabrication problems exist for cooled radial rotors.

The design process to arrive at an acceptable cooled radial rotor is an iterative one that must accommodate the competing interests of aerodynamics, heat transfer, structural integrity, and life requirements. The final proof-of-concept must be verified by performance, structural, and endurance testing to uncover any problem areas. This and the following lecture will review the present state-of-the-art as it exists today in the United States. The areas that will be covered are (1) aerodynamic performance considerations, (2) analytical heat transfer and cooling design procedures, and (3) fabrication technology.

AERODYNAMIC PERFORMANCE CONSIDERATIONS

There is a substantial amount of information in the open literature (see, e.g., refs. 1 to 6) on the selection of design parameters for radial turbines. Most of the literature deals with minimizing the aerodynamic losses to obtain a high efficiency and reports the results of either experimental or analytical studies of uncooled turbines. In those studies the turbine operating temperature was generally at a level so that the rotor stresses, although important, were not a major impediment to the designer. The aerodynamicist had considerable latitude in choosing design parameters that were expected to result in high turbine efficiency.

The general design procedure for a cooled radial turbine is similar, but material stresses and temperatures take on an increased importance in arriving at a final design. The turbine

efficiency is no longer the primary figure of merit; instead, the cooled radial turbine must be designed as a total system. The objective is to arrive at the lowest aerodynamic loss design while accommodating the necessary structural and geometric compromises required for acceptable material stress and temperature levels. In this section will be reviewed some limitations placed on the choice of design parameters and the effects of those constraints on the aerodynamic performance.

A common method of selecting a nominal value of the rotor tip speed for a given work requirement is to use the blade-jet speed ratio, U_{tip}/V_{jet}. In this dimensionless parameter, U_{tip} is the blade speed at the inducer, and V_{jet} is the jet or spouting velocity corresponding to the ideal expansion from inlet total to exit static conditions across the turbine. The variation of turbine efficiency, obtained either by experiment or analysis, reaches a maximum at a U_{tip}/V_{jet} near 0.7, although the level may change for different designs. A typical curve for a given turbine (taken from ref. 7) is shown in figure 1. Most high-temperature turbines are also high-work turbines. Therefore, as the specific work increases, the blade speed must also increase to obtain maximum efficiency. However, blade speed is limited because disk stress increases by the blade speed squared. Lowering the blade-jet speed ratio from 0.7 to 0.65 or even to 0.6 does not cause a large drop in efficiency but can significantly reduce centrifugal stress. This is a compromise well worth considering.

Turbines with radial-element blades are usually designed with some incidence that provides optimum flow conditions at the rotor inlet. This optimum incidence condition is analogous to the *slip* factor developed by Stanitz (ref. 8) for centrifugal compressors. Channel flow analyses have shown that the flow stagnation streamline is properly aligned with the blade leading edge when the inlet flow is at the optimum angle. The optimum angle is a function of blade loading and can be determined by the relationship

$$V_{u1}/U_{tip}=1 - (2/n)$$

where V_{u1} is the tangential velocity at the rotor inlet and n is the number of blades. An example of the use of this relationship for a high- work cooled turbine is shown in figure 2. The figure shows that blade speeds of 2175 to 2300 ft/sec (660 to 700 m/sec) were required to obtain the optimum inlet flow angle. Based on previous design studies of radial turbines, the allowable tip speed for this design was expected to be between 1800 and 2000 ft/sec (550 and 610 m/sec). At these reduced speeds there would exist substantial positive incidence. This incidence condition is often the case for tip-speed-limited high-work turbines. To reduce the large incidence loss, inlet-to-exit work split was adjusted to reduce the total losses between rotor-inlet incidence and exit swirl. Since the downstream ducting and subsequent turbine stages were not defined for this research exercise, it was assumed that the rotor-exit tangential kinetic energy was lost. The optimization study conducted included not only changes in the vector diagrams but also a preliminary estimate of rotor stress and temperature levels. The results of the study indicated that a total minimum loss occurred at a tip speed of 1880 ft/sec (575 m/sec) for a rotor with 14 blades. The final design efficiency of 0.86 was less than the peak efficiency, calculated without any structural constraints, but higher than that calculated with the high inlet incidence.

The axial width of the rotor blade at the inlet is another design variable that affects the blade and rotor disk stresses. A reduction in blade width reduces the centrifugal stresses as a result of the lower blade weight. At the same time, for a given inlet relative flow angle, a reduction in blade width increases the absolute flow angle and reduces the rotor reaction. This may reduce the efficiency due to increased endwall losses caused by thickening boundary layers. An example of the change in selected rotor flow conditions with a change in blade width is given in table I. Again, a compromise must be made by trading reduced blade and disk stresses for a possible reduction in turbine performance.

Most radial rotors have between 10 and 20 blades. Reducing the number of rotor blades has the obvious effect of reducing the disk stresses and coolant flow. It is also clear that as the number of blades is reduced, the blade surface friction decreases, but the possibility of local flow separation increases. The fearsome result of a large flow separation has lead designers to add blades when in doubt. The author knows of no reported study that defines the optimum number

TABLE I.— EFFECT OF CHANGES IN ROTOR INLET BLADE WIDTH

Blade width	Beta(1)	Alpha(1)	M_1	$M_{r,1}$	$M_{r,2t}$	$M_{r,2h}$	Alpha(2)	Reaction (a)	Centrifugal stress, P/A (a)
0.304	15	70	1.180	.418	.786	.511	0	Inc.	Inc.
.379	15	75	1.122	.301	.786	.511	0	Inc.	Inc.
.536	15	80	1.080	.194	.786	.511	0	Inc.	Inc.

[a]Increasing.

of radial-rotor blades; however, the results of one experimental study (ref. 9) are shown in figure 3. These results show that the efficiency did not peak for the highest number of blades tested. The results of Mizumachi (ref. 10 and reported in ref. 11) showed a similar trend. In that study the maximum efficiency was reached with 17 blades. In evaluating the desirability of a given number of rotor blades, the increases in aerodynamic performance must be balanced against the increased coolant flow required. In an engine application this tradeoff would be assessed as part of the engine cycle analysis.

The shape of the rotor-hub contour affects both the blade passage aerodynamics and the disk stress. A small-diameter hub reduces the hub rim velocity and therefore the disk stress level. The benefit of the reduced hub diameter is lessened by the increase in blade radial length resulting in higher blade hub stress. Aerodynamically, a smaller hub diameter aggravates the diffusing flow along the hub. The results of a design study (ref. 12) are shown in figure 4. A flow analysis of the original hub contour indicated a large flow separation along the hub near the blade suction surface. Additional hub contours were analyzed to reduce or eliminate this potential loss source. Contour A substantially reduced the separated area, and contour B indicated no separated flow. Changes in other streamlines in the blade passage that resulted from the revised hub were insignificant and did not indicate any separation. However, the study also showed significant increases in disk stress caused by the hub modifications. A tradeoff was reached by selecting contour A as the best compromise between performance and structural considerations.

The trailing-edge thickness of a cooled rotor blade can become quite large when it must contain cooling-air passages or coolant-discharge passages. The required trailing-edge thickness can result in a hub blockage over 50 percent. An analysis of the rotor trailing-edge mixing loss for a cooled turbine (ref. 13), having a blockage that varied from 21 percent at the tip to 53 percent at the hub, resulted in an estimated decrease in overall efficiency of 0.9 point. Fortunately, extremely thick trailing edges can be avoided, for example, by ejecting the cooling air in a film upstream of the trailing edge or along the blade shroud in the clearance gap. Examples of these will be shown and discussed later.

The blade leading edge has also been considered for ejection of spent coolant. A water table experiment was conducted (ref. 9) to study the effect of exhausting the coolant at that location. A combination of air bubbles and dyed water was used to trace the coolant and primary flows. Figure 5 shows the relative streamline patterns of the two flows at different

rotor speeds. The sketches show the flow pattern at the rotor tip for negative incidence (at N = 30 rpm), for near-zero incidence (at N = 22 rpm), and for a small, positive incidence (at N = 19 rpm), both with and without coolant flow. With the flow approaching the blade at zero incidence, the discharging of coolant did not change the primary flow pattern significantly. However, at negative and positive incidence, the areas of flow separation with zero coolant were increased by the coolant ejection. As stated earlier, tip-speed-limited rotors would likely have positive blade incidence. The result of these qualitative tests suggests that any flow separation already present due to positive incidence may be increased by the discharging coolant with the possible result of increased rotor loss.

Most modern radial-turbine designs have fully scalloped rotors, i.e., the backplate material between the blades down to hub is removed. This has the effect of removing material that must be structurally supported by the disk thus lowering the disk stress. The efficiency penalty associated with a fully scalloped rotor is not considered severe because the loss attributed to the backface clearance is mostly offset by the reduced backplate disk friction.

Cooling technology developed for axial turbine nozzles is often used directly in the design of radial-turbine vanes. As with the rotor, it is desirable to reduce the number of vanes to the minimum, consistent with acceptable aerodynamic performance, to reduce the amount of coolant flow. Design parameters such as blade solidity can be used to define the minimum vane number, but, if the number is reduced below established experience levels, the design should be verified by experiment. In some cases the vane trailing-edge thickness may need to be increased to allow for coolant flow ejection and/or improved heat conduction from the vanes to the sidewalls. Thus, as the vane number is reduced increases in trailing-edge thickness will have less of a detrimental effect on vane exit mixing losses. The results of an experiment comparing the turbine efficiency changes of thin trailing-edge vanes, which are typical of an un cooled nozzle, and of thick trailing-edge vanes, which are typical of a cooled nozzle, are shown in figure 6. The efficiency change in the figure is shown as a function of the trailing-edge thickness-to-throat ratio. With only two data points, it was assumed that the loss varied linearly. For the turbine design under evaluation, the data indicated a performance penalty of 1/4 point. A penalty this small can usually be offset by the advantages of higher cycle pressure ratio and turbine-inlet temperature.

The preceding paragraphs reviewed some of the tradeoffs necessary between aerodynamic performance and other design disciplines to achieve a viable, cooled radial-turbine design. Most of these compromises trade some turbine performance for a lowering of blade and disk stresses. Other tradeoffs included reducing the number of vanes and blades to reduce the amount of coolant flow and, finally, changes in the blade geometry to accommodate the coolant flow. Although none of these tradeoffs increase the turbine aerodynamic performance, they are not necessarily additive and, therefore, may not cause a major performance decrease. Several cooled radial turbines have been designed with design efficiencies between 0.86 and 0.88. Performance data have been obtained for several of these research turbines. Figure 7 shows data taken at 100 percent design speed for a NASA cooled radial turbine. These data were taken without coolant flow, but more recent tests with coolant show no dropoff in performance. This initial test was made with large rotor clearances to preclude any mechanical rubs. Analysis of the data (ref. 14) shows that two-thirds of the rotor loss is clearance loss. The turbine design efficiency is expected to exceed the goal of 0.87, at the design pressure ratio of 4.0, when run with design rotor clearances. Performance tests of other research cooled turbines have shown similar positive results. The conclusion that should be drawn from these performance tests is that compromises made in the aerodynamic design to lower rotor stresses and to accommodate the addition of cooling air can be managed without disastrous effects on performance.

HEAT TRANSFER AND STRUCTURAL ANALYSIS

The development of an acceptable cooled radial-turbine design requires detailed and accurate knowledge of the temperature and stress distributions throughout the rotor. An analytical model is usually developed by dividing the rotor into a number of wedges equal to the number of blades. Boundary conditions are then applied as heat loads and surface temperatures and the temperature distribution calculated. With these calculated rotor temperatures and with the blade external and internal pressure loads, a structural analysis is performed. From this analysis rotor stress distributions are obtained which, in turn, are used with material strength properties to make a life evaluation. Any shortfall in turbine life or, conversely, an overly conservative design requires changes in blade geometry, cooling configuration, and/or disk metal distribution. Because of the interdependence of the many factors that affect the results, an iterative procedure is followed. Initially, simplified analytical procedures are used to minimize the time and effort to assess a design change. After the design has evolved to the final configuration, more detailed and complex methods may be used.

The accuracy of the results obtained from the mechanical analysis is directly dependent on the fidelity of the model being analyzed and the accuracy of the applied heat loads. Calculations of the heat-transfer characteristics of cooled turbine blades require complex analyses aided by empirical correlations of experimental data. The accurate calculation of the external and internal heat-transfer coefficients is necessary to achieve an efficient cooling design. In this section will be reviewed methods to determine the heat flux from the hot gas to the blade, the heat removal by the internal coolant, the role played by the empirical correlations, and the present efforts underway to refine these analyses.

Cooling considerations.— Circumferential gradients in turbine-inlet temperature can be considered averaged out because of the rotor rotation, but spanwise gradients cannot. Figure 8 shows several turbine spanwise temperature variations that are used by the turbine designer. A vane may be subjected to a local hot spot where the temperature is considerably above the averaged turbine-inlet temperature. This is the condition that the vane must be designed to withstand. The rotor, however, "sees" the relative temperature, which may be less than the average inlet temperature. These differences in design temperature are a function of both the combustor characteristics and the turbine velocity diagrams and vary for each application.

An important temperature concept used in determining the local heat flux is the adiabatic wall temperature. This temperature is illustrated in figure 9(a), which depicts the flow of a fluid over an insulated surface, i.e., zero heat flux between the fluid and the surface. The fluid static and stagnation temperatures are T_g and T_g', respectively. As one approaches the insulated surface in the Y direction there is a rise in the static temperature until it reaches the surface value, T_{aw}. This surface value is called the adiabatic wall temperature. The adiabatic wall temperature is greater than the free-stream static temperature but not quite equal to the stagnation temperature. The adiabatic wall temperature can be calculated from the equation

$$T_{aw} = T_g + R(V_{fs}^2/2gJc_p)$$

where R is the recovery factor, which may be approximated by $R = Pr^{1/2}$ for laminar flow, and $R = Pr^{1/3}$ for turbulent flow (Pr is the Prandtl number.) For flow in a turbine the recovering factor is usually about 0.9. High-speed flow experiments have shown that the flow of heat between a fluid and a surface, like that shown in figure 9(b), depends on the difference between the adiabatic wall temperature and the surface temperature according to the equation

$$q = h_g(T_{aw} - T_{wo})$$

The problem in determining the heat flux to the surface is to find a suitable expression for the heat-transfer coefficient, h_g.

Figure 10 shows the basic methods used to air cool turbine components. Of these methods, convection, impingement, and film cooling have been used in cooling designs of radial-turbine rotors. Examples of these will be discussed later in this presentation. Combining cooling methods often results in greater cooling effectiveness. The net gain by combining both convection and film cooling in a given design is shown in figure 11. Here, blade surface temperatures are given for convection cooling only, film cooling only, and combined convection and film cooling, all at the same turbine-inlet temperature and total coolant flow rate. Except near the film ejection hole, the combined effect of convection and film cooling significantly lowers the wall temperature below that of using either cooling method separately.

Hot-side convection.— To evaluate the heat flow from the hot gas to the blade, the convective heat-transfer coefficients must be determined over the blade surface. The method frequently used in a first-order design is to obtain values for h_g from correlations developed for flow over a flat plate. For turbulent flow over a flat plate without film cooling, the following expression is given for the local Nusselt number

$$Nu_x = h_g x/k_g = 0.0296 Re_x^{0.8} Pr^{1/3}$$

where Re_x is the Reynolds number based on the distance x. The local temperature and temperature-dependent fluid properties are evaluated from local relative flow conditions. Since the local temperature varies in the thermal boundary layer, a temperature correction is applied to the fluid properties. Two schemes commonly used are the temperature-ratio method and the reference-temperature method. These methods are easily used and explained in many sources (e.g., ref. 15).

If localized film cooling is present, the heat flux equation is altered by replacing the adiabatic wall temperature by the local film temperature:

$$q = h_g(T_f - T_{wo})$$

The variation in film temperature with distance from the injection hole has been experimentally determined for a variety of hole geometries and orientations (see fig. 12). These data have been correlated in dimensionless form by the film effectiveness, E_f, such that

$$E_f = (T_{aw} - T_f)/(T_{aw} - T_c)$$

where T_f is the film temperature and T_c is the coolant temperature at ejection. Although the heat-transfer coefficient near the film-injection location is altered by the film, the effect is damped out quickly and so no change is made to the heat-transfer coefficient.

The blade leading edge is usually treated as a cylinder in crossflow. It is in this region of the blade that the highest heat-transfer coefficient is found. An expression for the Nusselt number for the leading edge (from ref. 16) is

$$Nu_{le} = h_g d/k_g = C Re_d^{0.5} Pr^{0.4}$$

where the coefficient C varies from about 1. to 1.6, depending on the turbulent intensity and where Re_d is the Reynolds number based on the blade leading-edge diameter.

Along the backface of the rotor the heat-transfer coefficients are obtained separately for (1) the scalloped region and (2) the rotor surface below the scallops, i.e, the disk face. In the scalloped region the heat-transfer coefficients may be assumed to be the average of the blade suction and pressure surface values along the hub streamline. The disk face can be modeled as

an enclosed rotating disk next to a stationary wall. An equation (taken from ref. 17) that may be used for this area is

$$Nu_{df} = h_g r/k_g = 0.0195(\omega \rho r^2/\mu)$$

where ω is the rotational speed and r is the radius.

The above simplified equations using flat-plate approximations can be replaced by more refined and accurate approaches. One method is to solve the boundary-layer equations either by integral or finite-difference techniques. Also, work is in progress to further develop two- and three-dimensional full-channel viscous-flow codes having adequate spatial resolution at the blade boundaries to calculate the local heat flux. The penalty for more accuracy is, of course, the increased complexity of the calculation. Often, the more sophisticated methods are not warranted in the early stages of a design.

Coolant-side convection.— There can be many different internal cooling configurations used to promote heat transfer and cooling of the rotor blade, and for that reason, it is impossible to review each convection cooling scheme. In principle the approach is similar to that used for the hot-side convection. The coolant heat-transfer coefficient, h_c, and the local coolant temperature, T_c, must be evaluated for use in the heat-flux equation

$$q = h_c(T_{wi}-T_c)$$

where T_{wi} is the coolant-side wall temperature. The problem is complicated because the coolant flow and pressure distributions must be known before h_c can be determined. An iterative cycle is necessary. The calculations are made by setting up a flow network for a given cooling configuration and solving conservation equations of momentum, mass, and energy. Once the amount of coolant for a given region of the blade is determined, empirical correlations for the particular cooling scheme can be used to obtain h_c. The procedure is repeated until the changes of successive calculations are within a specified tolerance.

For design purposes the coolant flow is usually modeled one dimensionally. One such coolant flow code is described in reference 18. Although written to analyze coolant configurations in radial-turbine rotors, the method is general and can be applied to other types of cooled components. In the code the momentum and energy equations are integrated along a defined flow path to calculate the coolant flow rate, temperature, pressure, and internal heat-transfer coefficients. The analysis accounts for area changes and centrifugal effects. Fluid friction and heat addition are calculated using correlations based on local flow conditions. A limitation of the analysis is that only those geometries consisting of a single flow passage with a single inlet and exit can be analyzed.

Reference 19 describes an extension of the above code. The latter code can handle many passage geometries, allows for branching of the flow, has additional heat-transfer correlations, and can calculate the heat-transfer differences between the leading (suction) and trailing (pressure) blade surfaces. Heat-transfer enhancement devices include wall turbulators, cross-channel pins, longitudinal fins, and impingement cooling. The report also contains an extensive bibliography of heat-transfer references. Although the code is operational at NASA Lewis it has not yet been released.

One-dimensional coolant analyses are widely used in the design of cooled turbine blades because of their relative ease of use and short computer run times. However, these codes do not calculate the internal flow and thermal conditions with the same precision as that achieved by passage flow analyses of the hot-gas stream. To overcome this deficiency, three-dimensional viscous codes are also being developed to analyze the coolant flow. Two research efforts are discussed briefly.

A study was recently completed by Adapco (ref. 20) of the coolant flow in the NASA

cooled radial turbine. The internal cooling configuration in shown in figure 13, and the grid used for the numerical model is shown in figure 14. The flow solver used was the STARCD code. Results of the calculation to model a reduced temperature experiment are shown in figures 15 to 17. Examination of the velocity vector field (fig. 15), shows significant regions of flow separation and recirculation. This kind of information is not available with a one-dimensional analysis. Also, the coolant flow distribution from the viscous calculation is much different from that obtained with an early one-dimensional analysis, although a more recent one-dimensional analysis made with the code of reference 19 agreed better. The verification of the STARCD results will be made with experimental data. A second, parallel effort at the Carnegie Mellon University is also nearing completion. The grid package GRID2D/3D, developed to model complex cooling geometries, is described in reference 21. The coolant flow solution is not yet complete but the approach being taken is reported in reference 22. As these and other three-dimensional coolant codes are developed and verified, more accurate flow calculations of cooling schemes will result.

Rotor mechanical analysis.— The detailed procedure followed to structurally analyze the NASA cooled radial turbine for the reduced temperature experiment and the results obtained are reported in reference 23. The finite-element model of the rotor wedge segment is shown in figure 18. With the heat loads specified for this model, the heat-conduction program, SINDA, was used to calculate the rotor temperature distribution, and the NASTRAN code was used to obtain the stress distribution. These results at the suction surface are shown in figure 19.

COOLED ROTOR CONCEPTS AND FABRICATION

In the remainder of this presentation will be reviewed the major programs sponsored by the US Army and NASA in the past 20 years to develop cooled radial rotor technology. The emphasis of these programs was on rotor fabrication. Most efforts culminated in rotor hardware demonstrations and produced a large amount of new fabrication technology. Although no cooled radial turbine entered into service, an appreciable amount of the technology was integrated into other high-temperature applications. Current research in this area is directed at improving the analytical and predictive tools of hot-gas and coolant-side heat transfer. These analytical tools will be equally useful to all types of turbines.

Monorotor.— The monorotor was conceived as a way to use low-cost components to operate at high engine cycle temperatures. The radial monorotor (ref. 24), was designed to operate at a rotor-inlet temperature of 2200 °F (1205 °C) without internal rotor cooling. The turbine cooling was to be accomplished by direct conduction to the centrifugal compressor which served as a heat sink. The compressor and turbine were to be integrally cast back-to-back as a single unit (see fig. 20). Supplementary cooling of the turbine was provided by controlled leakage flowing from the compressor tip into the turbine and down the hub disk surface. This coolant film is shown in figure 21. The turbine nozzle and compressor diffuser were also integrated to form a monostator, the hot turbine nozzle being cooled by conduction to the diffuser vanes as well as internal impingement flow. The stator cooling air was ejected at the vane trailing edge.

The effect of compressor heating was estimated by evaluating a simple gas-turbine cycle having a 10:1 pressure ratio and a constant maximum temperature. It was estimated that the heat flow to the compressor would have the effect of raising the compressor-inlet temperature 14 °F (8 °C). This, in turn, would reduce the compression process efficiency two points and require a 2.7 percent increase in compressor rotor tip speed to achieve the same pressure ratio as an unheated compressor. It also was estimated that the power output decreased by 3.2 percent and that the specific fuel consumption of the cycle increased by 2.2 percent.

Detailed thermal and structural analyses of the monorotor indicated significant tempera-

ture gradients and high thermal stresses. Temperature contours of the rotor, both with and without film cooling, are shown in figure 22. As would be expected, the film cooling is effective near the point of injection but then decays rapidly. The turbine blade in the exducer-shroud region shows an unchanging temperature, whether the film is present or not. The blade normal thickness and spanwise taper were increased to enhance heat conduction to the disk. The rotor stresses are given in figure 23. About two-thirds of the total stress is thermal stress caused by the high-temperature gradients. The highest stress, which occurred between the disk and compressor blades, was caused by the hot disk applying shear loading to the blade. Several areas in the rotor were had critical combinations of stress and metal temperature and would not meet the design life of 1000 hr. A decrease of 100 °F (55 °C) in rotor-inlet temperature was made for the final detailed monorotor design.

Two monorotors (fig. 24), were machined from Udimet 700 forgings for a series of mechanical tests. The tests included vibration and rotor spin tests and were made primarily to obtain data to confirm and calibrate analytical dynamic and finite-element stress models. The program was then concluded.

First internally cooled rotor.— One of the first attempts to design, build, and test an air-cooled radial turbine was carried out by Pratt & Whitney Aircraft (refs. 9 and 25), under Army sponsorship. The goal of the program was to demonstrate high aerodynamic performance and structural integrity of a cooled, radial turbine at hot engine conditions. The turbine was designed for a stator-inlet temperature of 2300 °F (1260 °C), a total efficiency of 0.875, gas flow of 5 lbm/sec (2.27 kg/sec), and a specific work of 220 Btu/lbm (5.1×10^5 J/kg). It was projected that the turbine would use less coolant and have a higher efficiency than an axial turbine designed for the same requirements.

The nozzle design was an integral casting of IN100, having 20 hollow vanes with cooling inserts. A cross section of the vane is shown in figure 25. Six percent of the primary flow, based on the nozzle inlet, was used to cool first the stationary sidewalls and then the vanes. One-half of the coolant flow cooled the turbine backplate and the other half cooled the shroud. After cooling the vanes, the spent cooling air was exhausted at the vane trailing edge. The vanes were designed for a hot spot of 2600 °F (1425 °C) and a 300-hr stress-rupture life.

The rotor, an investment casting of IN100, had 12 blades and was cooled with 3 percent cooling air. The rotor internal cooling details are shown in figure 26. The rotor coolant entry, below the exducer hub, was peculiar to the component rig only and would be located elsewhere in an engine. In this configuration, cooling air flows up to the blade tip where 1/2 percent is bled into the mainstream. This small amount provides a film layer for the leading edge. The remaining cooling air then turns 180°, flows inward, and is ejected on the blade suction surface. The internal cooling geometry is relatively simple without any pin fins, turbulators, or flow branching. The internal heat-transfer coefficients were calculated using standard turbulent pipe flow methods.

Concurrent with the design of the turbine was a fabrication study conducted to evaluate feasible methods of casting the turbine nozzle and rotor. Results showed that the nozzle could be cast as an integral assembly, but fabrication of the rotor was much more difficult. Trial rotors and IN100 test bars were cast by three casting vendors. Problems of two types showed up. Many of the cast rotors did not fill completely or had core shifts and blade "kiss out." Also, the test bars did not have the material properties required to meet the design life goals. A casting development program was required.

The casting development program had two objectives: (1) improving the yield and quality of integral castings and (2) investigating the potential of bicast rotors. Bicasting consisted of casting the blades individually (see fig. 27) and then casting a hub of the same material around the blade roots. Bicasting offered several advantages: (1) improved yield, (2) simplified blade inspection, and (3) better temperature control during the casting cool down. Controlled cool down results in desirable grain formation and improved material properties. A

problem encountered with the bicast rotors was incomplete bonding of the blades to the hub. Welding, mechanical attachments, and new inspection techniques were all used to help solve the bond problem. Both integral cast and bicast rotors were improved during the program but neither method produced rotors having design material properties, and final testing was conducted with structurally limited rotors. All hot testing was done with bicast rotors. A finished rotor is shown in figure 28.

A series of rig problems during the hot testing cut short the planned experimental program. The design conditions of 2300 °F (1260 °C) turbine-inlet temperature and 67 000 rpm at 18 atmospheres were not achieved. The maximum conditions reached were 2045 °F (1120 °C) and 53 000 rpm. A limited amount of aerodynamic data was obtained at the reduced operating conditions. From these data it was concluded that the turbine efficiency was between 0.86 and 0.89 at design conditions. Extrapolation of the cooling data to design conditions indicated that the cooling design was adequate for the turbine sidewalls but that data scatter and suspected leakage made an evaluation of the nozzle cooling design inconclusive. No cooling data were obtained for the rotor due to instrumentation failure.

Despite the experimental difficulties encountered at the end of the program, valuable information was obtained. The aerodynamic performance of a cooled radial turbine was shown to equal that of an uncooled design. The structural strength of integral castings can approach that of wrought material. The highest rotor burst speed was obtained with an integral casting. Bicasting offers a potentially attractive method to fabricate cooled rotors. Other lessons learned were also important. The yield rates of integrally cast rotors may preclude that method for obtaining cost effective components. And new inspection procedures are a necessity to verify bonded rotors.

Hot-isostatic-pressed, bonded rotor.— In 1976 several potential solutions to the cooled radial-rotor fabrication problem surfaced. Promising new manufacturing technologies were under study both at government laboratories and within the aerospace industry. Two Army contracts were awarded to build a prototype radial-turbine rotor that was structurally sound, cost effective, and had high performance. One recipient was Detroit Diesel/Allison-GM who proposed a hot isostatic pressure (HIP) procedure whereby a cast Mar-M247 air-cooled airfoil shell is joined to a PA101 powder metal hub. This approach provides the high strength creep-resistant blade material with a strong, fatigue-resistant ductile disk. Results of the design and fabrication phases are reported in references 11 and 26.

The turbine design conditions were rotor-inlet temperature of 2300 °F (1260 °C), gas flow of 5.35 lbm/sec (2.43 kg/sec), and a work output of 170 Btu/lbm (3.95×10^5 J/kg). The target efficiency was 0.86. The required design life for the turbine was 5000 hr, with 20 percent of that at maximum power and a low-cycle fatigue life of 6000 cycles. Since emphasis was placed on rotor manufacturing, a design of an air-cooled nozzle was not made.

The final rotor cooling design (fig. 29), had two smooth wall internal channels. Cooling air, equal to 3 percent of the mainstream, was taken on board through a series of holes on the rotor backface. Each hole fed one blade. Within the blade, the flow was divided with 2.3 percent going to the outer channel and 0.7 percent to the inner channel. Air exited the blade by a full-span-width slot on the pressure surface just upstream of the trailing edge. The disk outer rim was cooled by 1 percent film leakage that flowed down the hub to the rotor exit. The wheel bore was cooled with 1/2 percent coolant flow. No adverse effect on turbine efficiency was predicted from this cooling scheme. The minimum wall thickness was 0.025 in. (0.63 mm) in the blade tip. Also visible in figure 29 is the bond line between the blade shell and the disk plug.

The rotor blades were not cast individually but as an integral piece containing all the hollow blades and a hub ring. This procedure eliminated the difficult task of simultaneously bonding many individual blades but still had most of the advantages of single-blade casting. The thin ring of the blade shell provided additional areas for core support, minimizing core shift and blade kiss outs. Also, the absence of the disk during the casting pour allowed more

controlled cool down and improved material strength. Optimization of casting parameters resulted in increased yields of quality castings of the complex thin wall blade shell.

The powder metal hub was obtained as a net-shape part consolidated by HIP compaction. The rotor manufacturing procedure consisted of the following steps: Before rotor bonding both the blade shell and powder metal preform had their bond line surfaces accurately machined to form an interference fit upon assembly. A machined blade shell and hub are shown in figure 30. After shrink fitting the parts together the exposed shell-to-plug interfaces are vacuum brazed to seal out the high-temperature-and-pressure inert gas used during the HIP process. The parts are then bonded at 2215 °F (1210 °C) at 15 ksi (1030 bars) for 3 hr and heat treated. The procedure, with proper braze sealing, produced completely bonded rotors. A finished rotor is shown in figure 31, and a sectioned rotor showing a bond line is shown in figure 32.

An extensive test program was conducted with bonded test bars, test specimens taken from fabricated rotors, and spin tests of completed rotors. The tests consistently showed excellent material properties and bond lines stronger than the materials being joined. Rotors spun to destruction showed satisfactory results. and a 6000-cycle fatigue test at 1000 °F (540 °C) was completed successfully.

A nondestructive inspection method was also developed to test the quality of the bond joint. The technique is shown in figure 33. Ultrasonic energy is passed through water and directed at the bond line. If the bond is complete, the energy passes through and is scattered or reflected from the free surface to a receiver. If the bond is incomplete, the energy is reflected sooner. The time differential of the reflected signals is used to determine whether the reflection is from a bonding flaw or from the free surface. This technique detected flaws of 1/16 in. (1.6 mm) and was successful in locating a debond in one rotor. The technique was verified by sectioning the rotor.

Subsequent aerodynamic and heat-transfer tests, at reduced inlet temperature and pressure, have been made of this turbine. The aerodynamic test results demonstrated high performance and a design efficiency of 0.86. The heat-transfer tests were conducted at an inlet temperature of 500 °F (260 °C). Thin thermocouple wire was used to measure the blade metal temperature at design conditions. The test data were scaled to engine operating conditions using similarity relationships and compared with the design intent. The results indicated a need for improved understanding of the heat-transfer process in cooled blades and more accurate analytical tools, especially for the coolant flow.

Overall, the program was very successful. It demonstrated a viable manufacturing process for obtaining consistent, high-quality cooled radial rotors and the value of the ultrasonic inspection technique to evaluate bond quality. It also showed excellent agreement between predicted and measured rotor stresses and demonstrated high turbine aerodynamic performance.

Laminated rotor.— Concurrent with the HIP-bonded rotor program, Garrett/AiResearch (refs. 13 and 27) also received an Army contract to design a cooled radial turbine to meet the same design requirements. The manufacturing approach used was the AiResearch laminate process. This approach uses thin sheet stock, with photoetched perforations, to form laminates for the rotor. When these laminates are properly designed, stacked, and bonded, the resulting blank has the internal cooling passages properly formed. The material between the blades is then machined away to form an air-cooled radial rotor.

The process allows for the design and manufacturing of very complex internal geometries but also has some compromises. The internal design of the laminated wheel is shown in figure 34. This final design evolved from several trial cooling configurations. The cooling air branches several times and follows a circuitous and serpentine path. There are numerous series and parallel passages, pin fins, and bleed holes in the circuit. The total amount of cooling air is 5.85 percent. Of this total, 0.3 percent cools the bore, 0.6 percent cools the rotor backface and the remainder, 4.95 percent cools the blade internally. One percent of the coolant leaves the blade near the blade inlet, and the remainder exits along the blade shroud. Ejecting the cooling air at

the trailing edge was considered but rejected because of the thick trailing edge required. Also, exhausting the flow in the shroud clearance gap may have the beneficial effect of reducing the clearance loss. The inherent internal roughness of the laminate causes the heat-transfer coefficients to be higher than that of smooth walls, but causes greater pressure drops. Experimental studies indicated that roughness effects increased the heat-transfer rate 140 percent and the flow friction factor 480 percent. The stacking of the laminates in the highly cambered exducer part of the blade can also cause cooling-air restriction. An extreme example of this condition is shown in the section through an exducer portion of a blade (fig. 35). The vertical lines represent the individual laminates, while the dark and light areas represent the blade wall (after the exterior blade shape is machined) and coolant passage, respectively. In this example the internal laminate steps essentially close the coolant passage. A later study (ref. 28) stated that thinner sheet stock and laser-angled machining can alleviate this problem.

In the original work the manufacturing process consisted of chemically milling 0.020 in. (0.5 mm) Astroloy sheet to a precise thickness and then photoetching each sheet. The radial wheel blank contained 141 laminates with 92 cooling passage configurations. The passages were accurately generated using computer-aided design (CAD) techniques. After photoetching, the laminates were cleaned and coated with a bonding medium. The laminates were stacked, bonded, and heat treated in a vacuum furnace at 2150 °F (1175 °C) for 2 hr under 100 psi (6.9 bars) pressure. The bonded stacks were then inspected for bond integrity, and test specimens removed for mechanical property tests. The stacks were premachined to expose the blade-air cooling holes to conduct coolant flow tests. After a blank passes all tests, it is final machined. The process is shown schematically in figure 36, and a finished rotor is shown in figure 37.

An extensive series of mechanical tests was performed on the laminated wheel. These consisted of a stress-coat test; a growth, overspeed, and burst test; and cyclic endurance tests. Results of these tests were positive and showed that the laminated rotor achieved design strength. Material testing also verified the high-strength characteristics of the bonded structure in the longitudinal direction and the reduced strength in the transverse direction. Fortunately, axial stresses that could propagate flaws along the bond line are generally quite low in a radial wheel.

This manufacturing technique has received very little attention in recent years. This may be due to casting technology advancements and the steady progress being made with ceramic rotors for small turbine applications.

Split-blade rotor.— The last of the government sponsored research programs to improve the fabrication technology of cooled rotors was awarded to Solar Turbines in the mid-1980's. This NASA contract built on the successes of the Army programs and had as its objectives (1) raising the temperature capability of radial rotors above previous design levels and (2) lowering rotor manufacturing cost. In the previous HIP-bonded rotor program, a rather simple internal coolant scheme was integrally cast with the blade. Heat-transfer tests of that configuration indicated that a more complex cooling design would be needed for higher turbine-inlet temperatures. The split-blade concept (refs. 29 and 30) was conceived as a way to obtain complex cooling configurations without increasing fabrication cost. In this concept the rotor is cast in two parts, an inducer section, or star wheel, and an exducer section. The blades of the inducer section are cast without any internal cooling passage geometry but with an open slot. The cooling circuit details are constructed independently from sheet metal and sintered powder and are subsequently bonded within the blade slots. The inducer is then joined to the exducer to form a rotor.

The design rotor-inlet temperature for this research turbine was 2800 °F (1540 °C). Other design requirements were gas flow of 5 lbm/sec (2.27 kg/sec), a total efficiency of 0.85 and a 1500-hr rotor life. A cross section of the rotor is shown in figure 38, and the two internal cooling circuits are shown in figure 39. The total cooling air for the rotor was 13 percent. Of this, 3 percent cools first the rotor backface and then the star wheel in a double pass circuit.

Some of the cooling air leaves the blade passage at the leading edge, but the bulk of the flow exits the blade at about midchord and provides a film for the exducer. Two percent of the cooling air cools the outer portion of the inducer backface and then film cools the rotor hub. The exducer internal flow is 7 percent, which flows through a serpentine passage and exhausts at the blade trailing edge. The remaining 1 percent provides film cooling for the exducer hub. Heat transfer is enhanced by staggered trip strips in the passage of the star wheel and by a variable density of pin fins in the exducer.

The division of the rotor into two sections results in uncambered blades in the inducer section and cambered, nearly axial blades in the exducer section. Both rotor sections were formed by investment casting. The ceramic cores used in the exducer were relatively short, and there were many suitable locations to secure the cores in the casting mold. The blade slots in the inducer casting were formed with flat, solid ceramic cores that were held along the blade shroud and inlet perimeter. Casting the rotor in parts with small, simple cores was done to improve casting yield. As mentioned earlier, the blade inducer section internal details were created separately with a steel carrier sheet. The carrier sheet had the coolant passage details, i.e., flow dividers and trip strips, machined into it using CAM software. The carrier cutouts were then filled with Inconel 625 inserts and a powder superalloy/braze mixture and then sintered. After machining the carriers and blade slots for a net fit, the carriers were vacuum electron-beam-welded into the blades slots. The cooling details are then HIP bonded to the parent material. Afterwards the carrier is leached out in an acid bath. A prepared star wheel and carrier assemblies are shown in figure 40 and a completed wheel is shown in figure 41.

This somewhat lengthy manufacturing procedure has the following advantages: (1) improved casting yield, because of the simpler geometry of the two rotor halves, (2) the capability to form complex internal cooling schemes and, (3) permits easy altering of the inducer cooling design by only changing the CAD/CAM software that generates both the carrier cutouts and inserts. Conversely, nondestructive inspection of the blade internal details and evaluating the bonding was not adequately solved. The results of radiographic inspection of the blades were generally inconclusive. Coolant flow rate and pressure loss tests made with two wheels did show very consistent flow among blades.

NASA radial turbine.— The current cooled radial-turbine program at NASA Lewis is not a fabrication program but rather has as the objective improving the analytical tools needed to design high-temperature turbines. The program includes improving the predictive capabilities of the hot-side and coolant-side flow fields and heat transfer. Many of the elements of the research program have been alluded to earlier in this paper. The development of the thermal and structural analysis (ref. 23), the generalized one-dimensional coolant flow code (ref. 19), the assessment of the Adapco three-dimensional viscous code as a coolant flow code (ref. 20), and the Carnegie Mellon University grid generation package (ref. 21) are recent publications from that research. Along with the analytical efforts is an experimental effort to obtain aerodynamic and heat-transfer data to assess and modify the analyses. Aerodynamic performance evaluation of the NASA cooled radial turbine is presently underway. Partial results have been reported in reference 14 (and earlier in this lecture). Cooling data are being acquired from a NASA Lewis laboratory static heat-transfer tunnel, a low-speed rotating model of a single blade of the cooled turbine, and from high-speed tests of the research turbine. Much of the data and results obtained will be equally applicable to axial turbines.

The cooled radial-research turbine was designed jointly by NASA Lewis and Allison (ref. 12). The design requirements were a rotor-inlet temperature of 2300 °F (1260 °C) with coolant design growth capability to 2500 °F (1370 °C), a gas flow of 4.56 lbm/sec (2.07 kg/sec), a work output of 186.8 Btu/lbm (4.34×10^5 J/kg), and a design efficiency of 0.86. The design was based on the successful dual-alloy Army rotor. Several coolant concepts were evaluated based on fabrication, cooling effectiveness, and research objectives. It was particularly important to achieve a cooling design with well-defined internal flow characteristics to ease the task of data

acquisition and verification of the analytical methods. A result of this consideration was a minimum of flow branching. The internal cooling flow was analyzed with a one-dimensional flow model that was available at that time. Figure 42 shows details of the final cooling configuration. All of the cooling air flows to the inducer at high velocity to increase the heat-transfer coefficients. This eliminates the need for heat-transfer enhancement devices. A decrease in coolant temperature is shown in the inward flowing leg. This occurs because the heat gained by the coolant is more than offset by the temperature drop resulting from the radius change. The placement of the pin fins at midchord was selected to create flow resistance in the radial direction forcing the flow to fill the exducer region more uniformly. The cooling air exits the blade on the pressure surface.

The rotor was designed to meet a 5000-hr life with 20 percent at maximum power conditions. Specifications were also set for creep, low-cycle fatigue, and burst margin. The maximum calculated temperature in the blade was 1640 °F (890 °C) and 1260 °F (680 °C) in the PA101 material. Mar M-247 was selected for the blade shell and PA101 powder metal for the disk plug. A photograph of a ceramic core is shown in figure 43.

Two rotors are under test at NASA Lewis: one solid and one hollow. The solid rotor is being used for detailed aerodynamic testing, including rotating blade-surface static pressures, and the cooled rotor (fig. 44) will be used for extensive heat-transfer testing. The rotors were scaled up 1.8 times the engine size to match an existing test facility. Tests are being conducted at an inlet temperature of 400 to 800 °F (200 to 425 °C) and at reduced pressure.

CONCLUDING REMARKS

Extensive technology advancement of high-temperature cooled radial turbines has been accomplished in the pass 20 years. It is safe to say that cooled radial turbines can be designed to produce high specific work output at safe rotor stress levels and to accommodate cooling considerations, such as reduced number of vanes and blades, without suffering major penalties in aerodynamic performance.

The methods used to analyze the cooling flow and heat transfer in internal cooling circuits rely heavily on one-dimensional approaches and flat-plate data. These methods are easy to use, but better analytical tools are needed to improve the cooling designs and increase cooling effectiveness. Research underway to develop two- and three-dimensional coolant viscous codes will aid in advancing this part of the design process, but detailed benchmark experimental data of actual designs is required to verify the computational codes.

Significant advances have been made in rotor manufacturing. Cooled radial-rotor fabrication, although perhaps still the most difficult task, is not the barrier it once was. Perhaps the real barrier to the use of high-temperature cooled radial turbines is finding a suitable application. For those applications where a small, high-temperature turbine is required, the choice of machines is usually between a cooled axial turbine or an uncooled ceramic turbine, either axial or mixed flow. Cooled radial turbines have so far not been seriously considered.

REFERENCES

1. Shepherd, D.G.: Principles of Turbomachinery. Macmillan Co., 1956.
2. Rodgers, C.: Efficiency and Performance Characteristics of Radial Turbines. SAE Paper 660754, 1966.
3. Lagneau, J.P.: Contribution to the Study of Advanced Small Radial Turbines. Int. Note 38, von Karman Institute of Fluid Dynamics, 1970.
4. Hiett, G.F.; and Johnson, I.H.: Experiments Concerning the Aerodynamic Performance of

Inward Flow Radial Turbines. Paper 13 presented at the Thermodynamics and Fluid Mechanics Convention, Inst. Mech. Eng., London, 1964.
5. Rohlik, H.: Analytical Determination of Radial Inflow Turbine Design Geometry for Maximum Efficiency. NASA TN D-4384, 1968.
6. Kofskey, M.G.; and Nusbaum, W.J.: Effects of Specific Speed on Experimental Performance of a Radial Inflow Turbine. NASA TN D-6605, 1972.
7. Futral, S.M.; and Wasserbauer, C.A.: Off-Design Performance Prediction with Experimental Verification for a Radial-Inflow Turbine. NASA TN D-2621, 1965.
8. Stanitz, J.D.: Some Theoretical Aerodynamic Investigations of Impellers in Radial and Mixed Flow Centrifugal Compressors. Trans. ASME, Vol. 74, No.4, 1952.
9. Calvert, G.S.; and Okapuu, U.: Design and Evaluation of a High Temperature Radial Turbine. USAAVLABS TR 68-69, 1969.
10. Mizumachi; Endo; and Kitano: A Study of Aerodynamic Characteristics of Rotating Blades in a Radial Inflow Turbine. JSME-7, 1971.
11. Ewing, B.A.; Monson, D.S.; and Lane, J.M.: U.S. Army/Detroit Diesel Allison High-Temperature Radial Turbine Demonstration. AIAA Paper 80-0301, 1980.
12. Snyder, P.H.; and Roelke, R.J.: The Design of an Air-Cooled Metallic High Temperature Radial Turbine. AIAA Paper 88-2872, 1988.
13. Vershure, R.W.; Large, G.D.; Meyer, L.J.; and Lane, J.M.: A Cooled Laminated Radial Turbine Technology Demonstration. AIAA Paper 80-0300, 1980.
14. Tirres, L.: A Comparison of the Analytical and Experimental Performance of the Solid Version of a Cooled Radial Rotor. AIAA Paper 91-2133, 1991.
15. Glassman, A.J.; ed.: Turbine Design and Application. NASA SP290, Vol 3, 1975.
16. Zukauskas, A.; and Ziugzda, J.: Heat Transfer of a Cylinder in Crossflow. Hemisphere Publishing Corp., 1985.
17. Kreith. F.: Principles of Heat Transfer. 2nd Edition, International Textbook Co., 1965.
18. Meitner, P.L.: Computer Code for Predicting Coolant Flow and Heat Transfer in Turbomachinery. NASA TP-2985, also AVSCOM TR 89-C-008, 1990.
19. Kumar, G.; Roelke, R.J.; and Meitner, P.L.: A Generalized One-Dimensional Computer Code for Turbomachinery Cooling Passage Flow Computations. AIAA 89-2574, 1989.
20. Three Dimensional Flow Analysis of the Internal Passage of a Cooled Radial Rotor. Adapco, Melville, NY, Final Report, 1991.
21. Steinthorsson, E.; Shih, T.I-P.; and Roelke, R.J.: GRID3D-v2: An Updated Version of the GRID2D/3D Computer Program for Generating Grid Systems in Complex Shaped Three-Dimensional Spatial Domains. NASA TM-103766, 1991.
22. Steinthorsson, E.; Shih, T.I-P.; and Roelke, R.J.: Computations of the Three-Dimensional Flow and Heat Transfer Within a Coolant Passage of a Radial Turbine Blade. AIAA 91-2238, 1991.
23. Kumar, G.N.; and DeAnna, R.G.: Development of a Thermal and Structural Analysis Procedure for Cooled Radial Turbines. ASME Paper 88-GT-18, 1988.
24. Rodgers, C.: Advanced Radial Inflow Turbine Rotor Program - Design and Dynamic Testing. (Solar-ER-2519, Solar Co., NASA Contract NAS3-18524) NASA CR-135080, 1976.
25. Calvert, G.S.; Beck, S.C.; and Okapuu, U.: Design and Experimental Evaluation of a High-Temperature Radial Turbine. USAAMRDL TR 71-20, 1971.
26. Monson, D.S.; and Ewing, B.A.: High-Temperature Radial Turbine Demonstration. USAAVRADCOM TR-80-D6, 1980.
27. Vershure, R.W.; Large, G.D.; Meyer, L.J.; and Egan, M.J.: Cooled Laminated Radial Turbine Demonstration Program. USAAVRADCOM TR-81-D7, 1981.
28. Large, G.D.; and Meyer, L.J.: Final Report—Cooled Variable-Area Radial Turbine Technology Program. NASA CR-165408, 1982.
29. Hammer, A.N.; Aigret, G.G.; Psichogios, T.P.; and Rodgers, C.: Fabrication of Cooled

Radial Turbine Rotor. (SR 86-R-4938, Solar Turbines, Inc.) NASA CR-179503, 1986.
30. Hammer, A.N.; Aigret, G.G.; Rodgers, C.: and Metcaffe, A.G.: Composite Casting/Bonding Construction of an Air-Cooled High Temperature Radial Turbine Wheel. SAE Paper 831519, 1983.

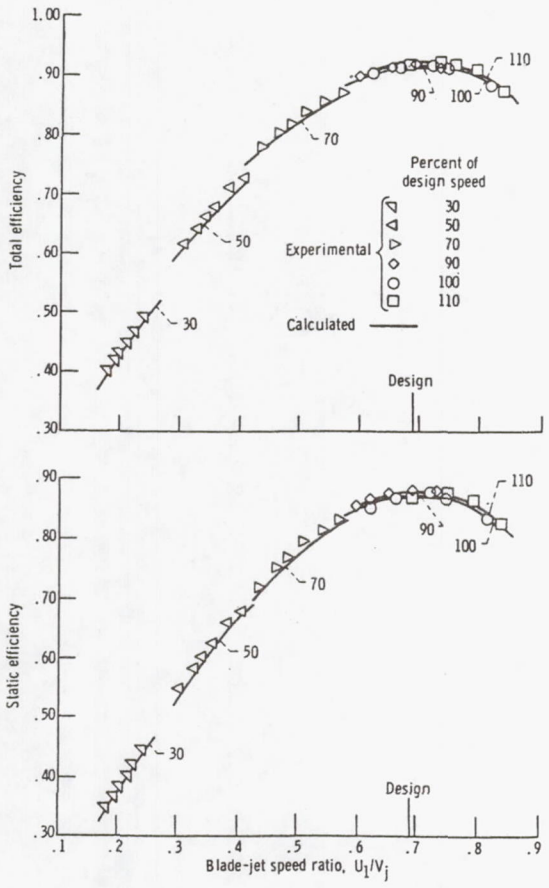

Figure 1. Radial turbine efficiency variation with blade-jet ratio.

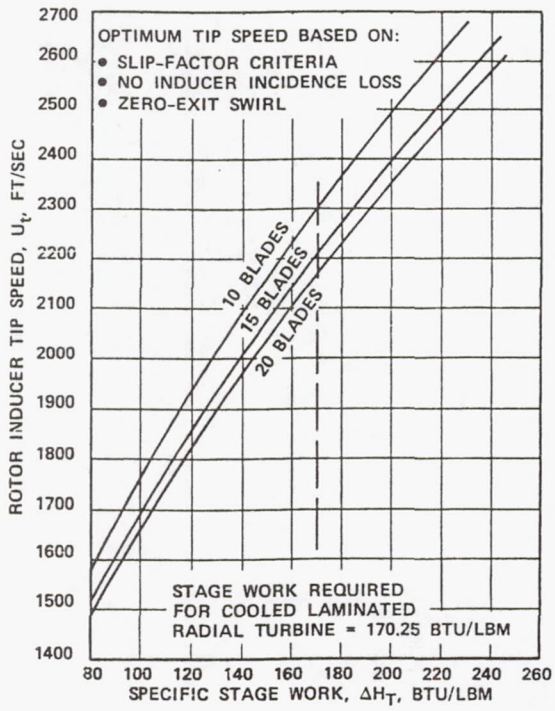

Figure 2. Optimum tip speed as a function of stage work and blade number.

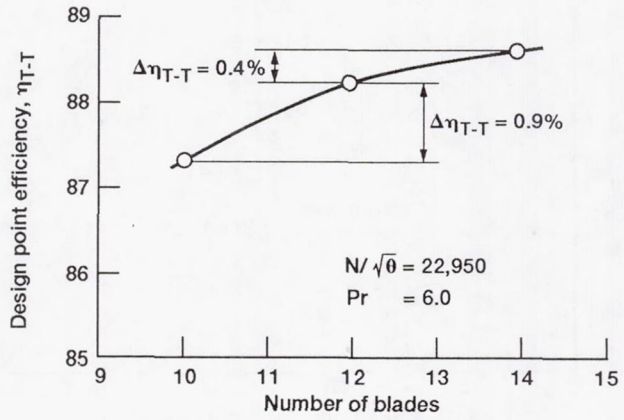

Figure 3.—Measured variation of turbine design point efficiency with number of rotor blades.

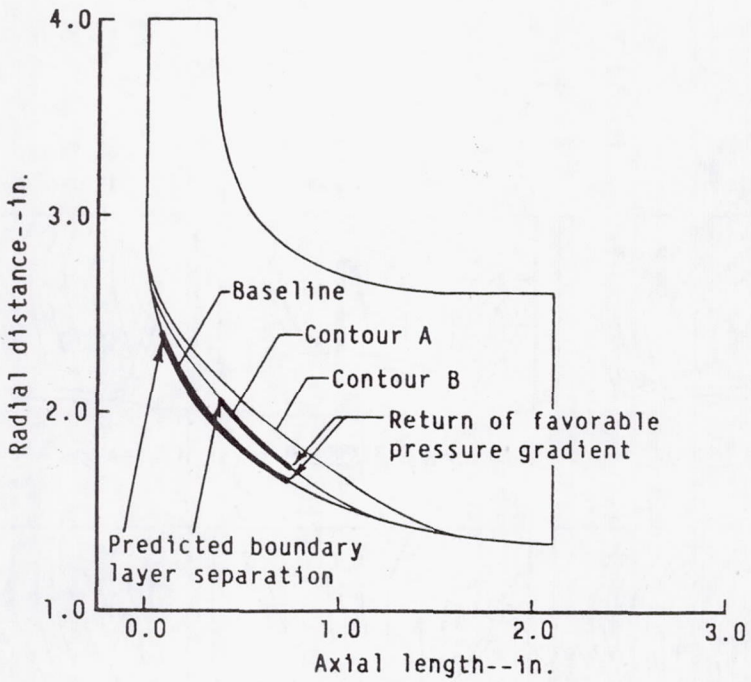

Figure 4(a). Alternate hub contours for improved rotor blade diffusion.

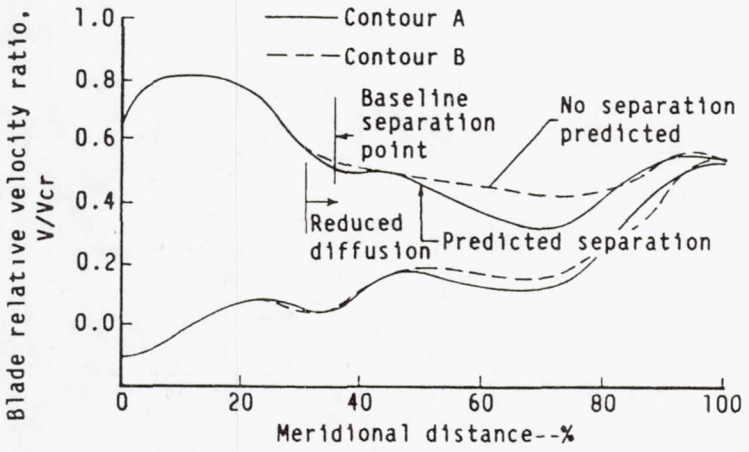

Figure 4(b). Changes in hub surface velocity with hub contouring.

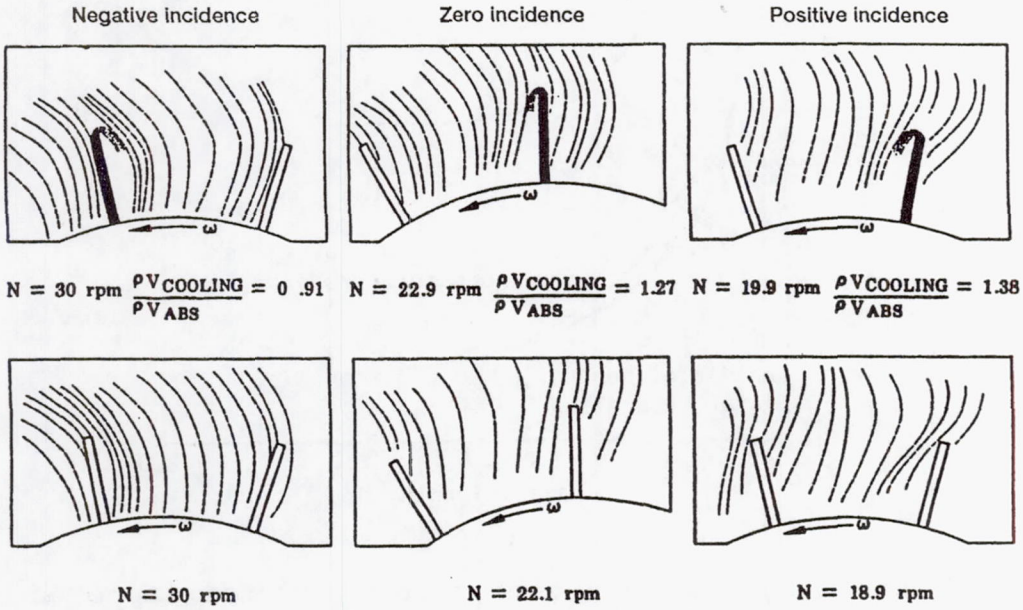

Figure 5.—Relative flow patterns with and without cooling air ejection at the rotor inducer.

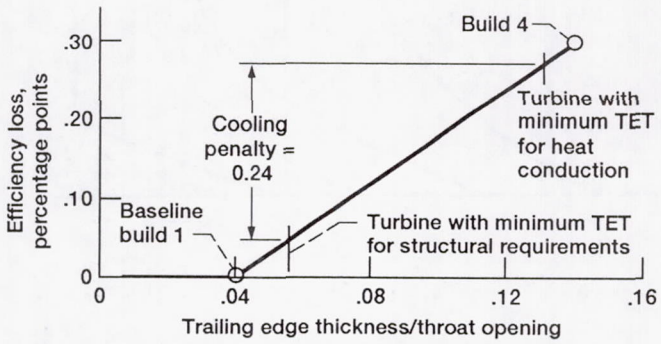

Figure 6.—Change in stage efficiency with TET/Throat ratio.

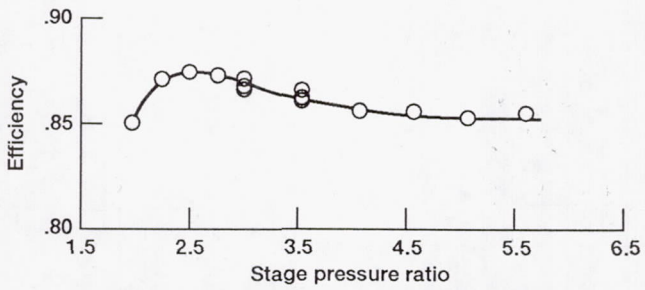

Figure 7.—Measured stage efficiency at 100 percent design rotor speed.

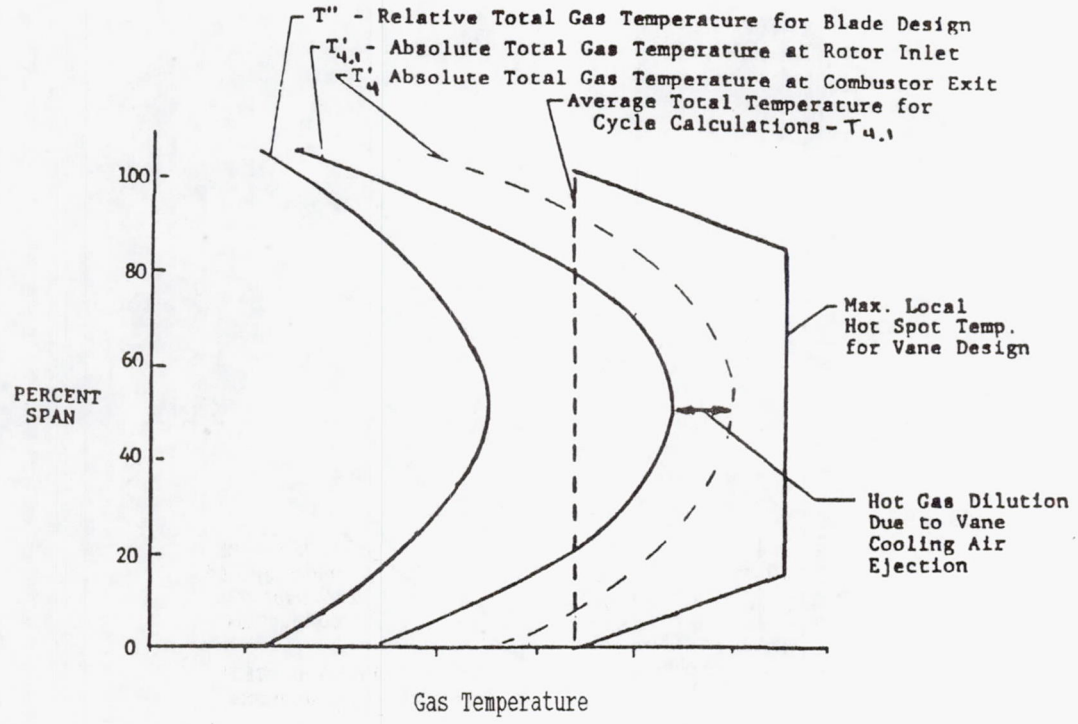

Figure 8. Spanwise variation in turbine gas temperature.

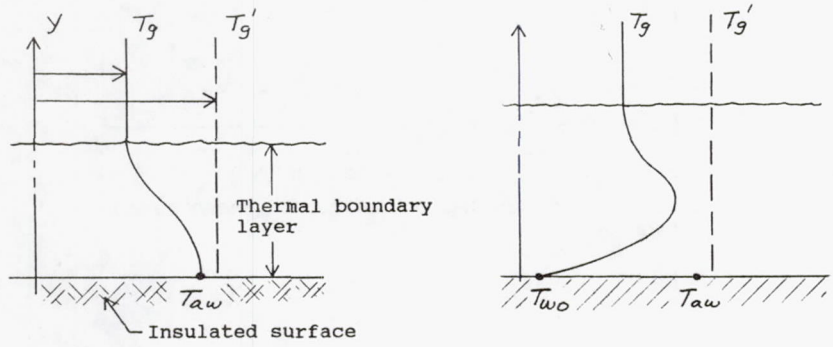

a) Adiabatic wall temperature.

b) Heat flow to surface.

Figure 9. Fluid temperatures near a surface.

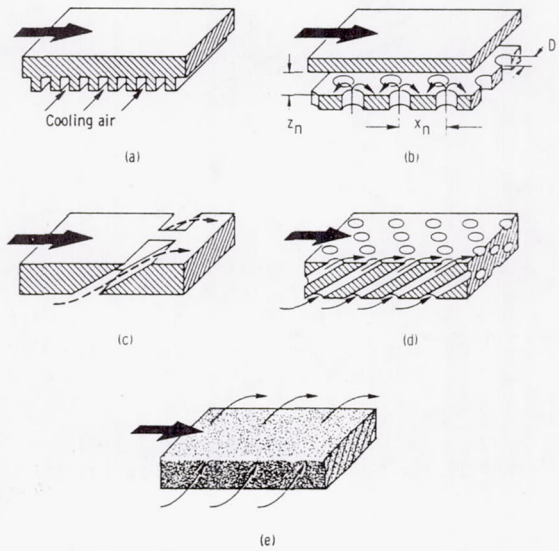

(a) Convection cooling.
(b) Impingement cooling.
(c) Film cooling.
(d) Full-coverage film cooling.
(e) Transpiration cooling.

Figure 10. Methods for turbine blade cooling.

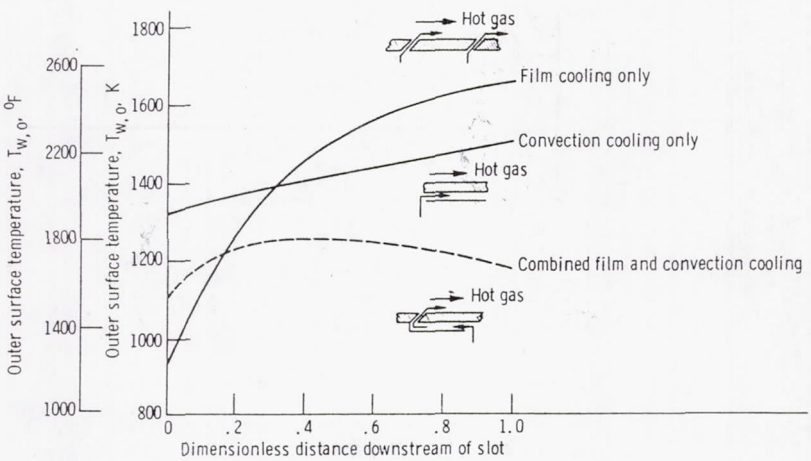

Figure 11. Effect of combining film and convection cooling. Constant flow rate.

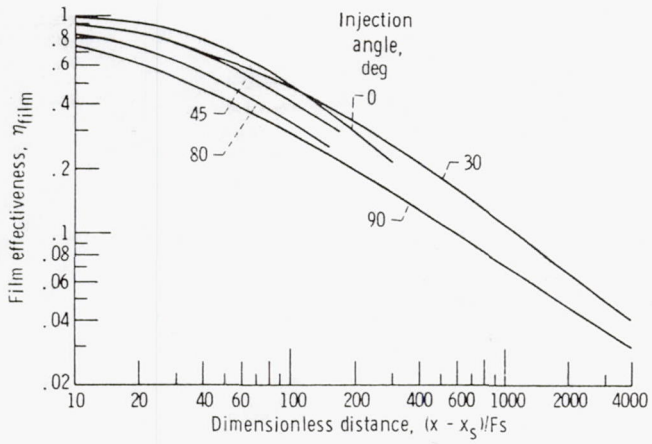

Figure 12. Film cooling effectiveness for slots.

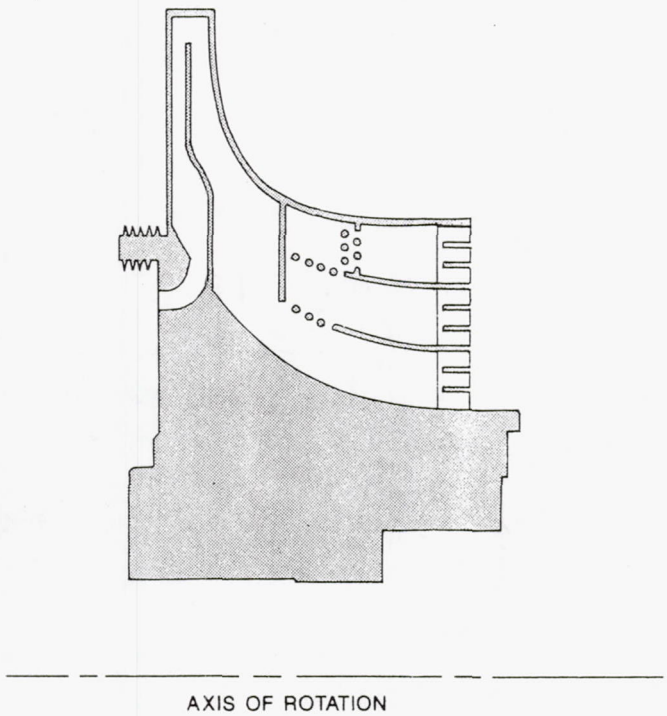

Figure 13. Cooling passage configuration of the NASA cooled radial turbine rotor.

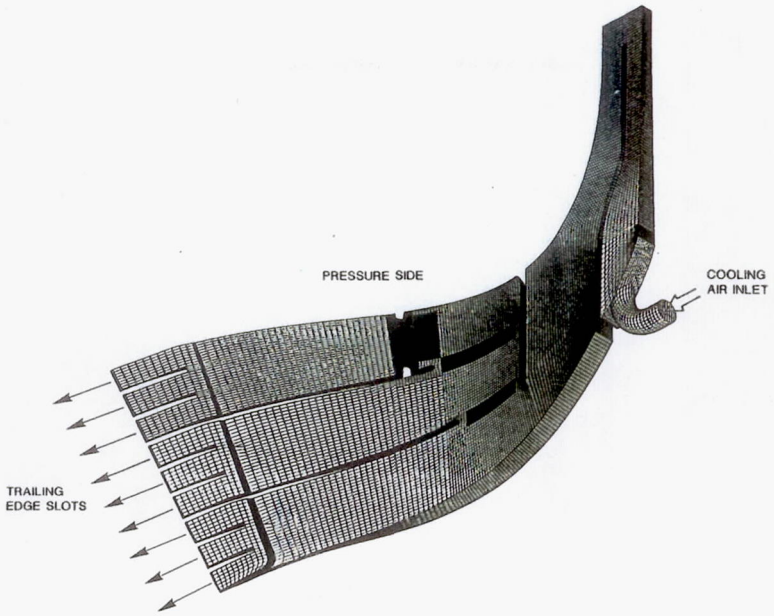

Figure 14. Internal passage numerical grid.

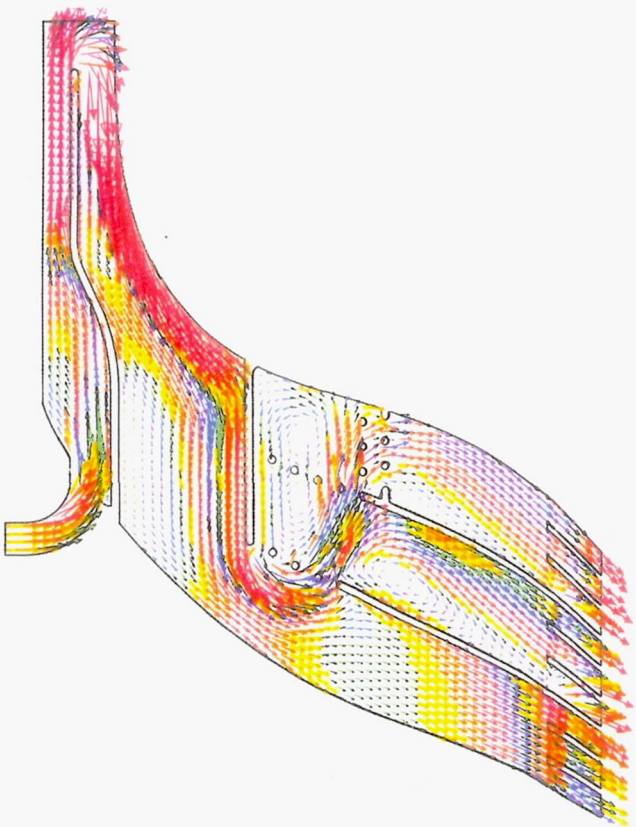

Figure 15. Coolant velocity vectors at midplane of internal passage.

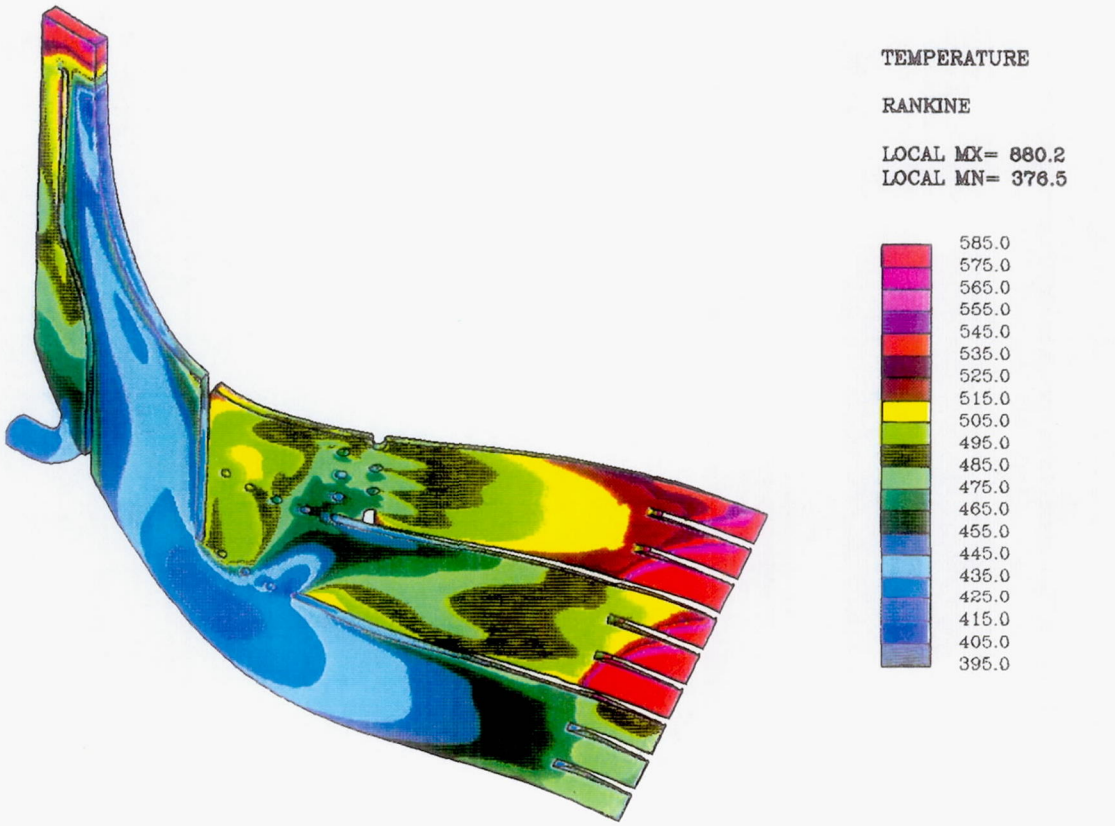

Figure 16. Coolant temperature at midplane of internal passage.

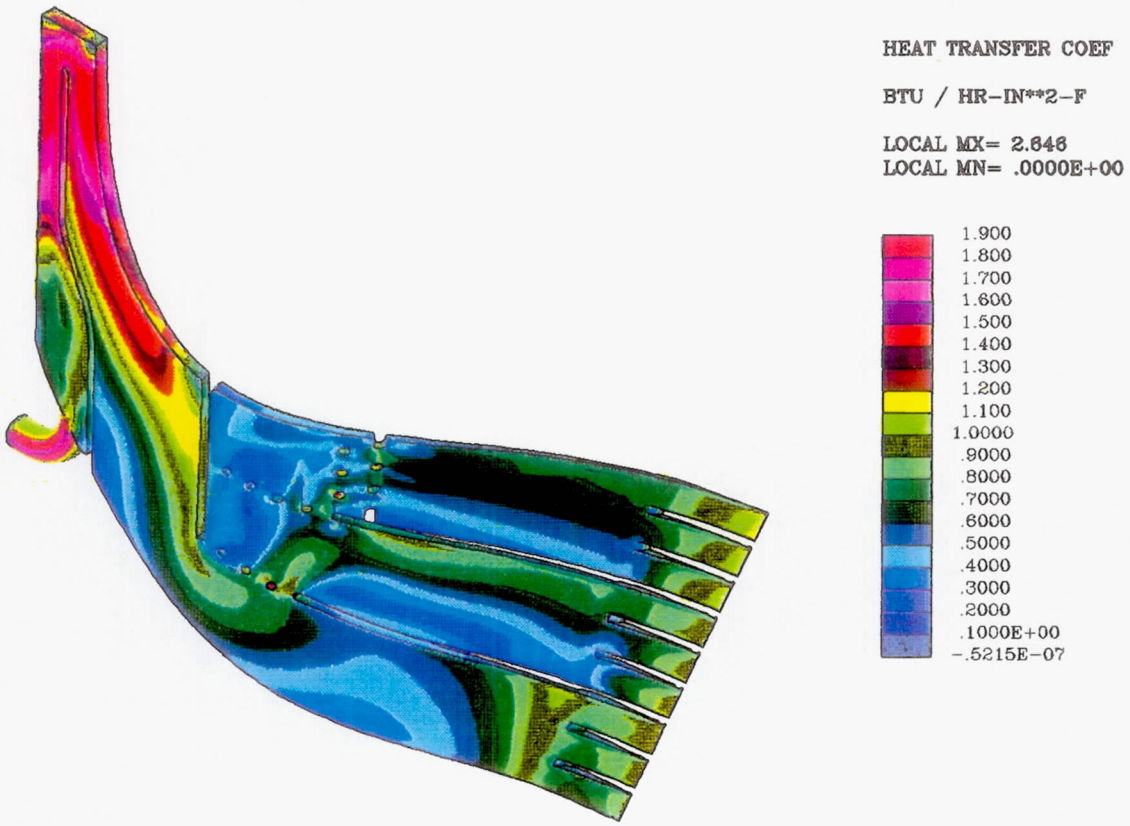

Figure 17. Internal heat transfer coefficients on pressure side.

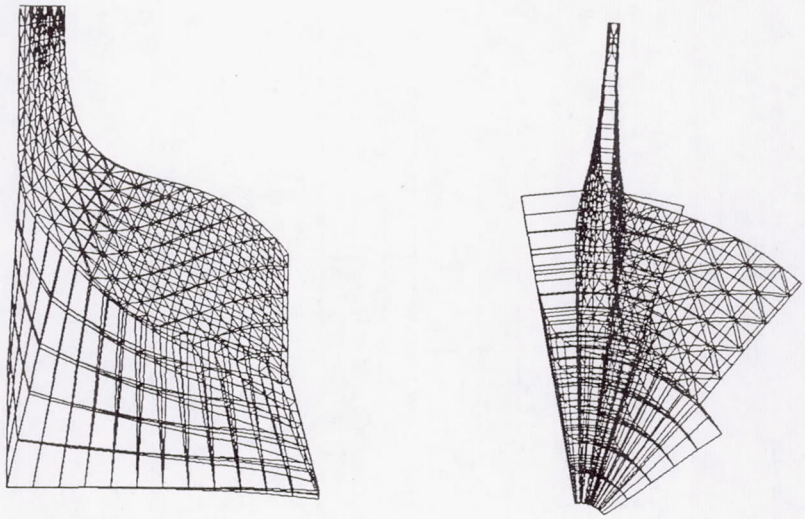

Figure 18. Finite element model.

CONTOUR LEVEL	TEMP (K)
A	395.
B	380.
C	365.
D	350.
E	335.
F	320.
G	305.
H	290.
I	275.
J	260.

CONTOUR LEVEL	STRESS (MPA)
A	360.
B	325.
C	290.
D	255.
E	220.
F	185.
G	150.
H	115.
I	80.
J	45.

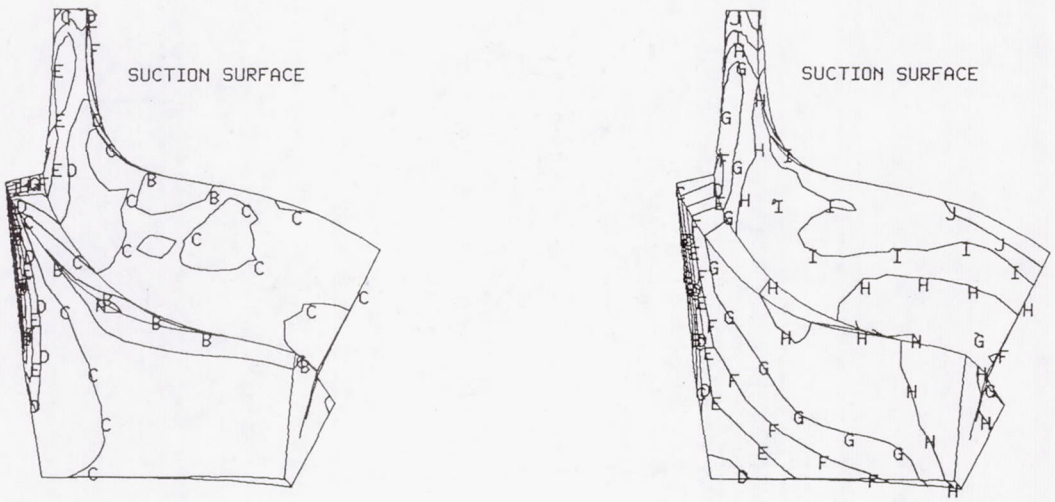

Figure 19. Rotor structural analysis results.

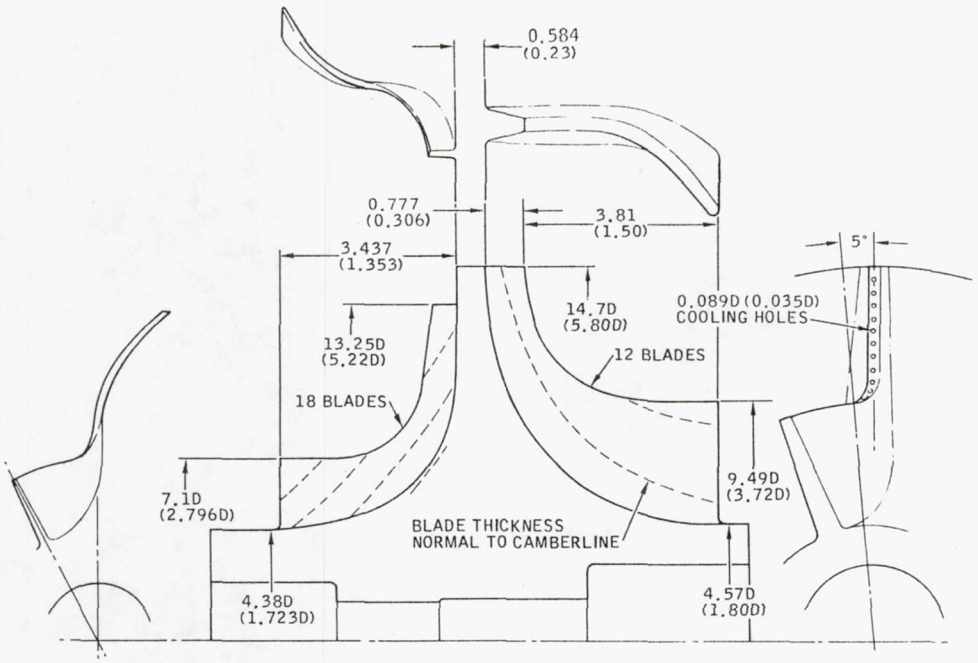

Figure 20. Monorotor geometry.

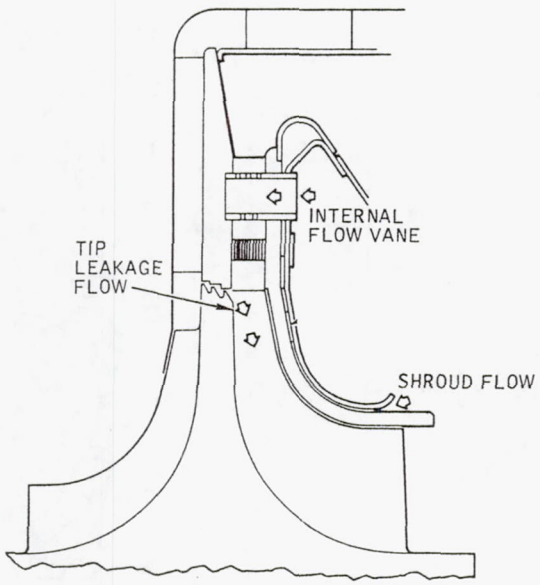

Figure 21. Monorotor assembly.

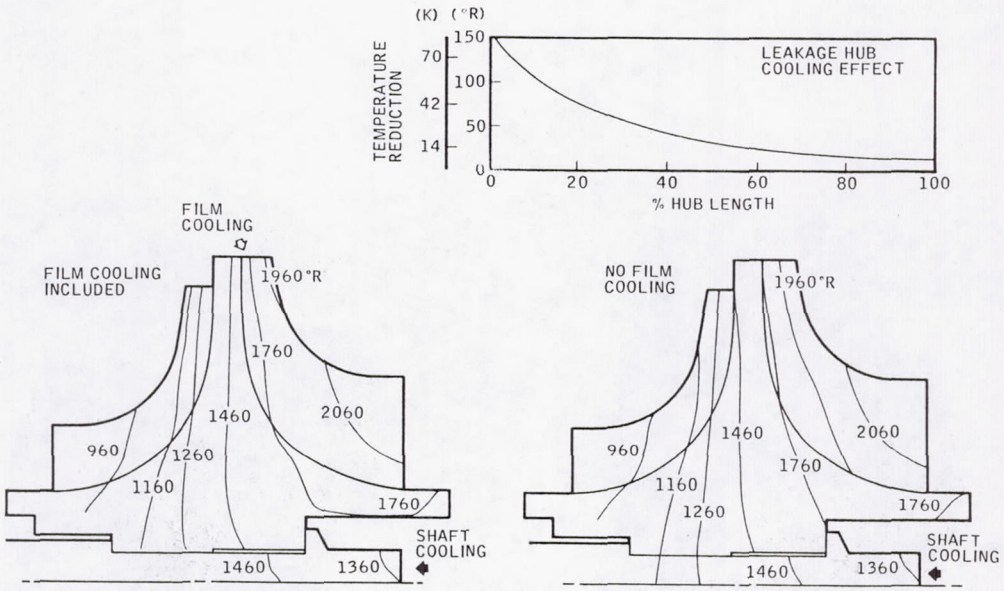

Figure 22. Monorotor temperature distribution.

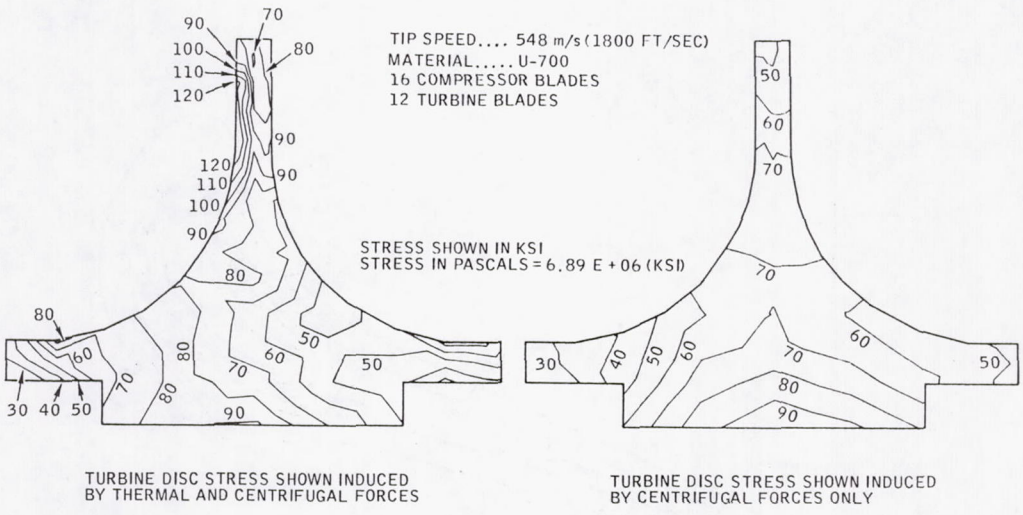

Figure 23. Disk stresses.

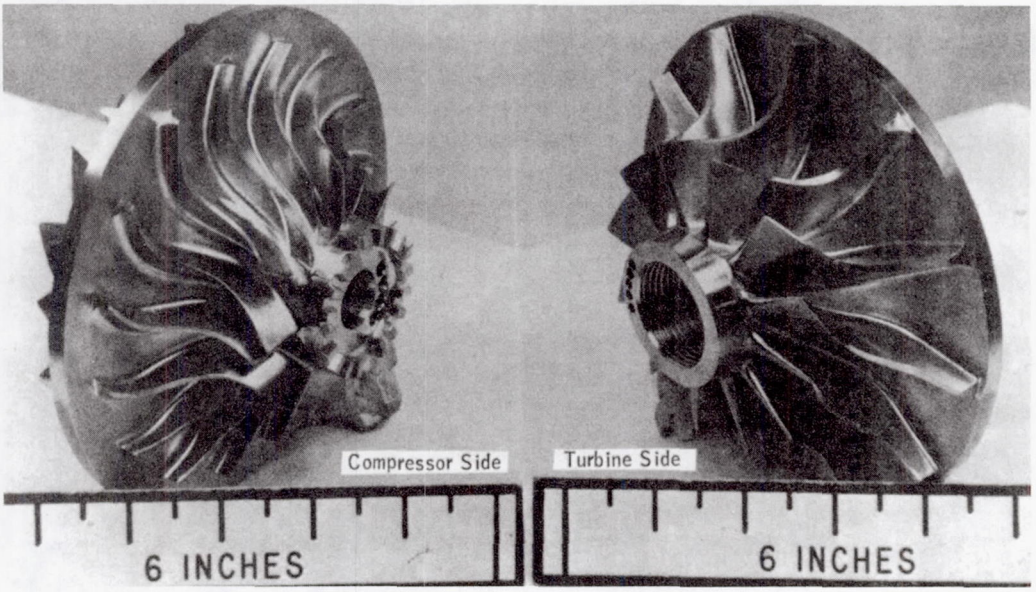

Figure 24. Finished monorotor.

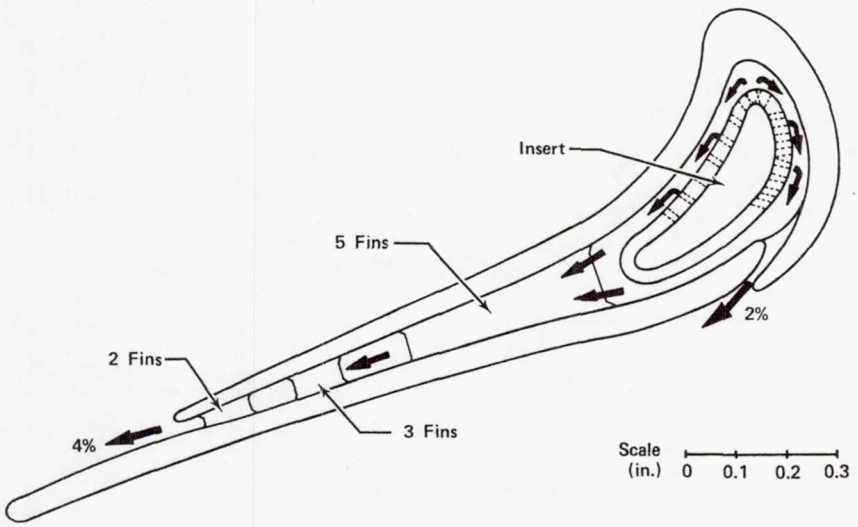

Figure 25. Nozzle vane cooling configuration.

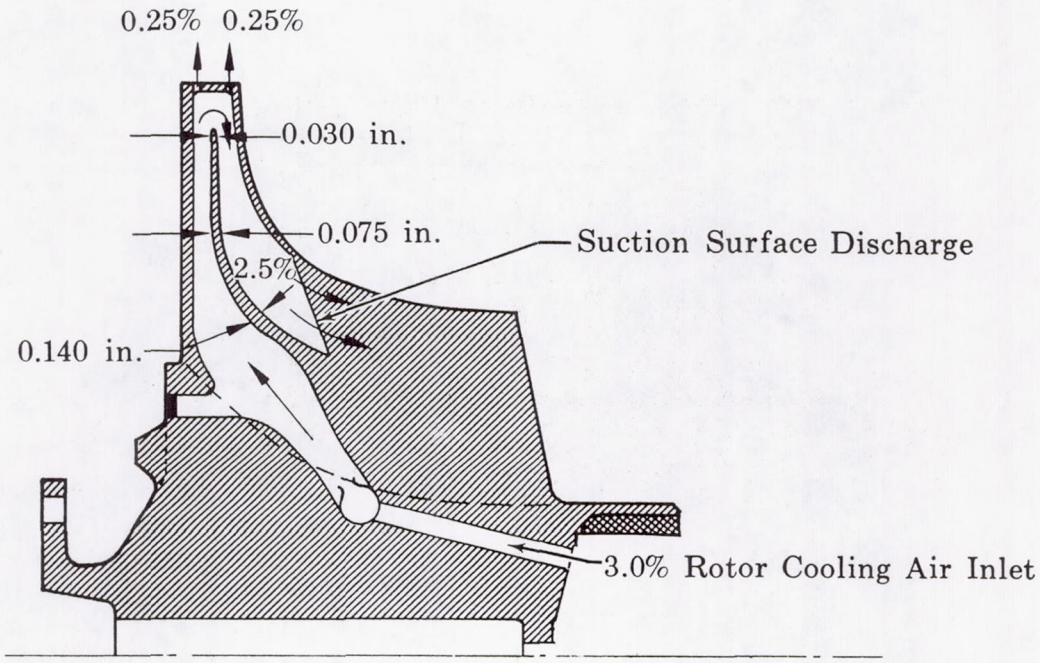

Figure 26. Rotor cooling configuration.

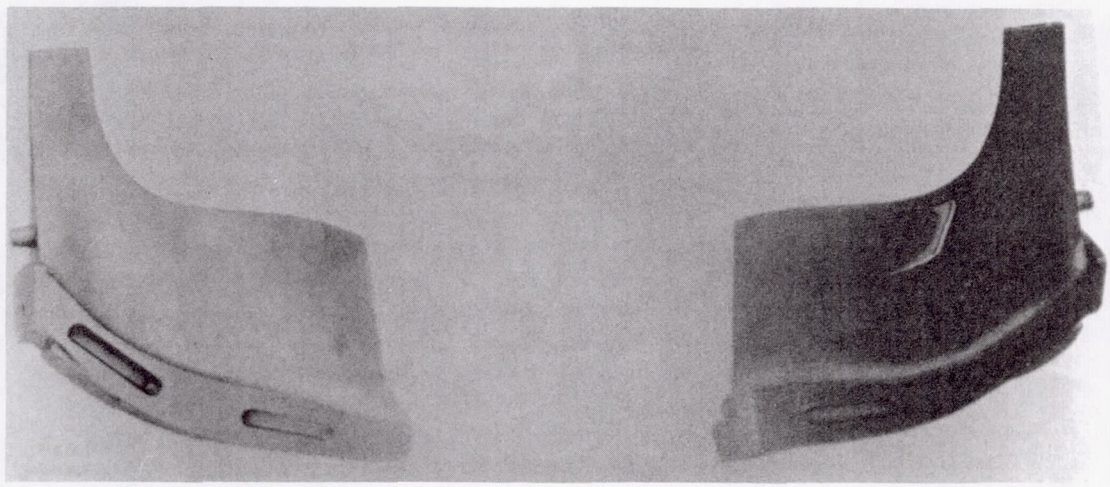

PWA 658 BLADE CASTING
(PRESSURE SIDE)

PWA 658 BLADE CASTING
(SUCTION SIDE)

Figure 27. Individual blade castings.

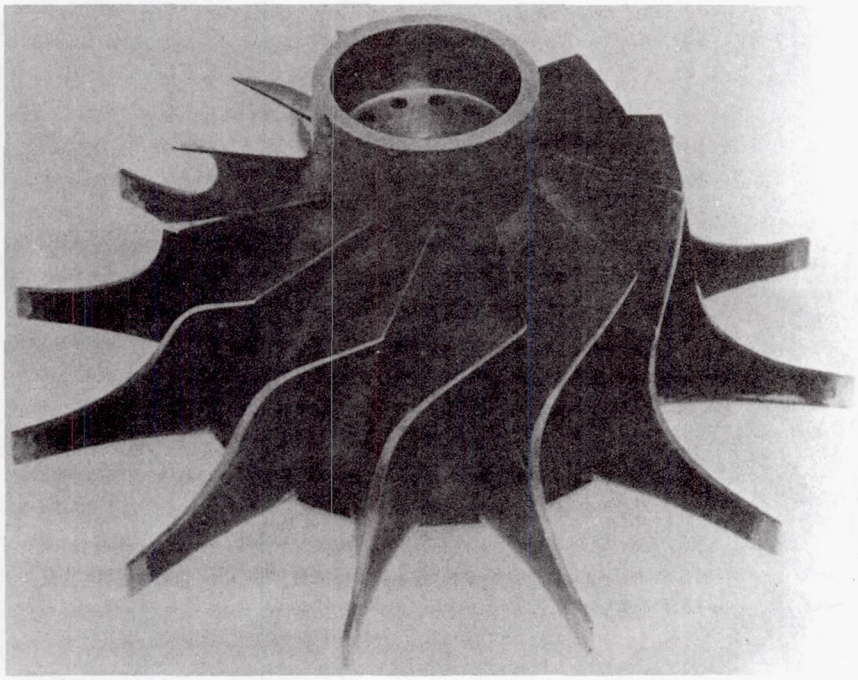

Figure 28. Finished rotor.

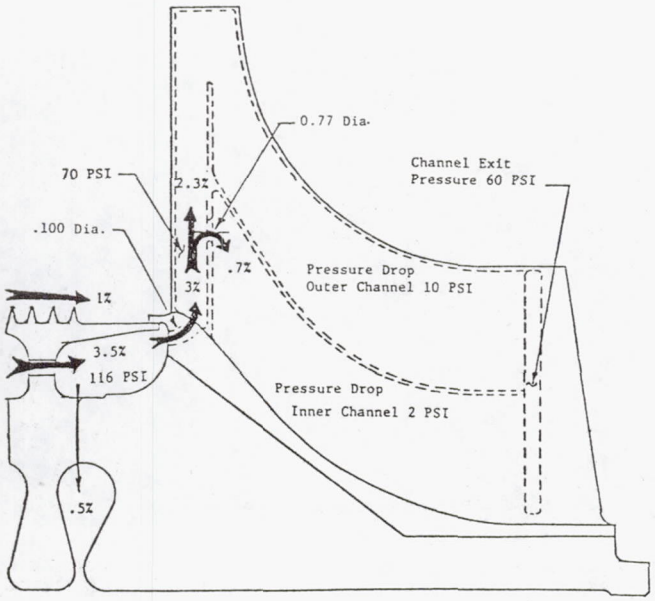

Figure 29. HIP bonded rotor cooling configuration.

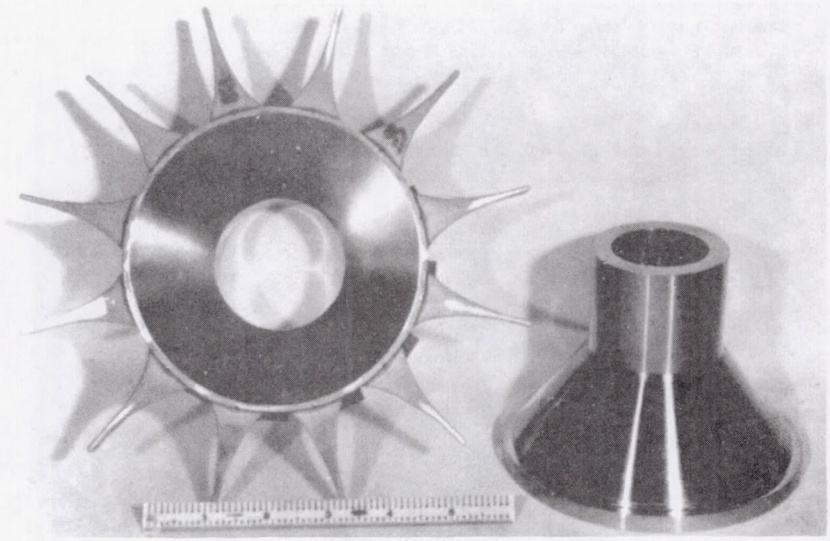

Figure 30. Machined blade shell and powder metal hub.

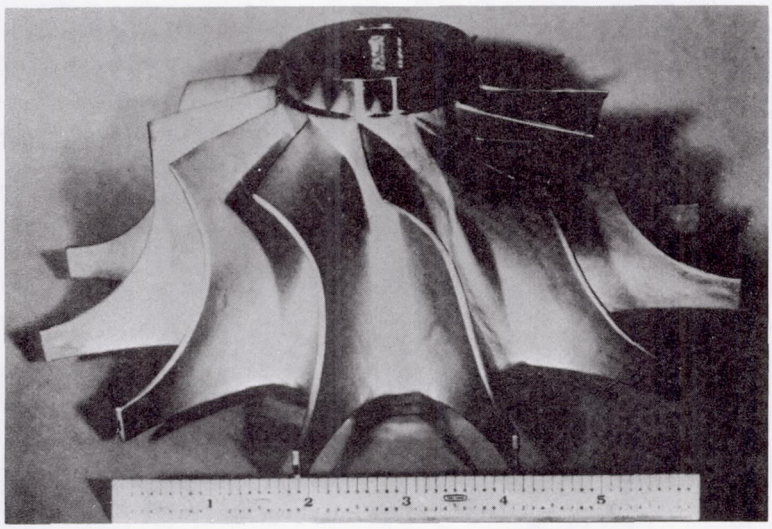

Figure 31. Finished HIP bonded rotor.

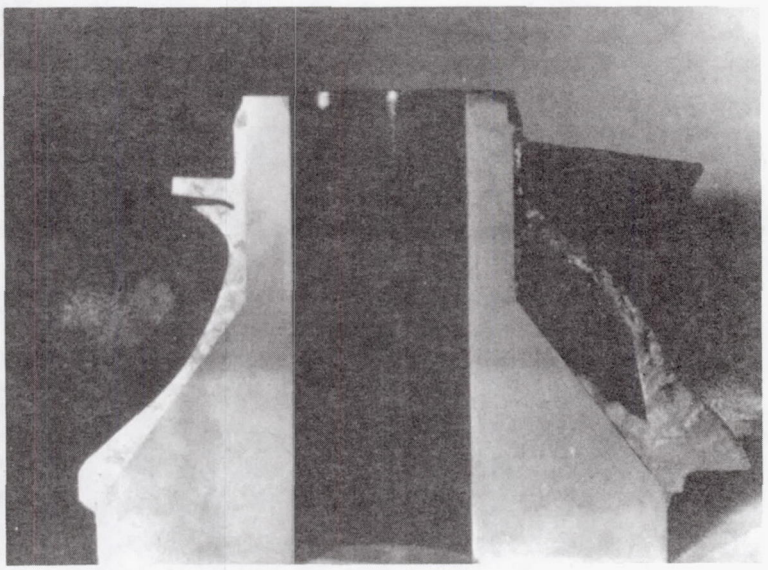

Figure 32. Rotor bond line; left bonded and right unbonded.

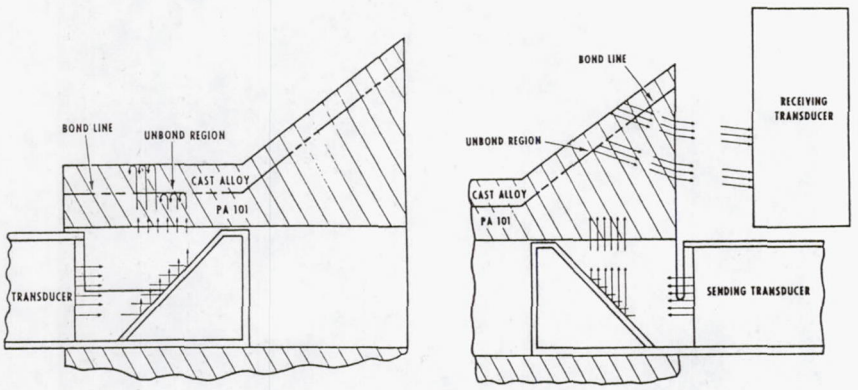

a. Cylindrical Section

b. Conical Section

Figure 33. Inspection technique for bonded rotor.

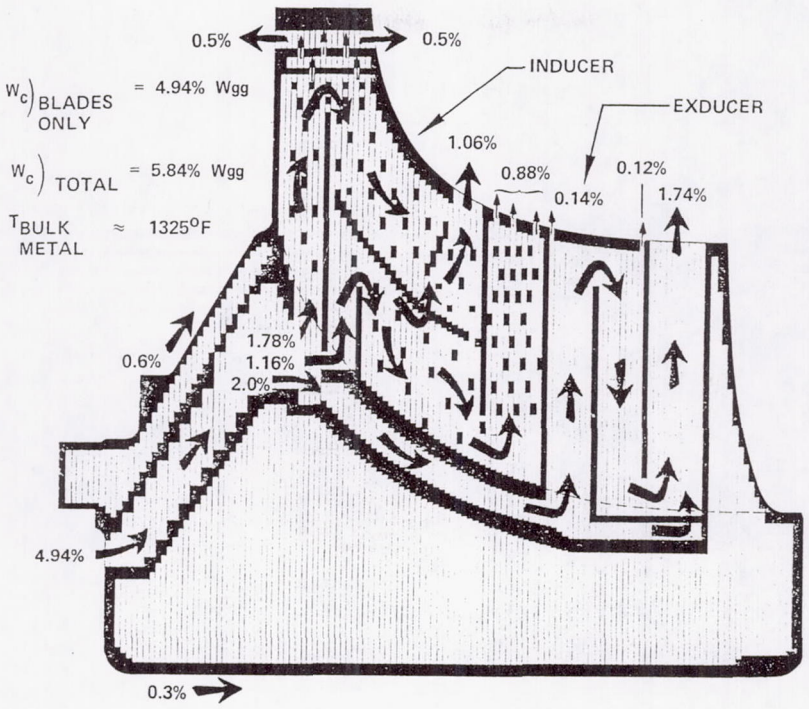

Figure 34. Laminated rotor cooling geometry.

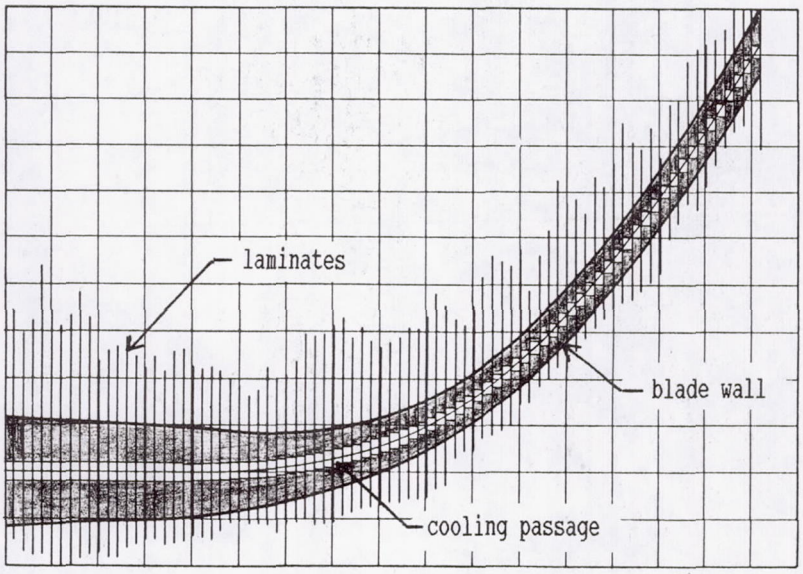

Figure 35. Laminate steps in cambered exducer section.

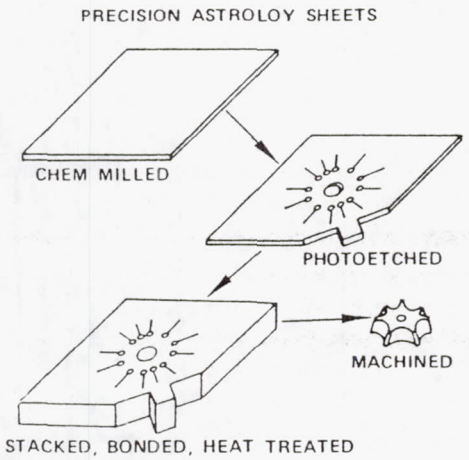

Figure 36. Laminate manufacturing process.

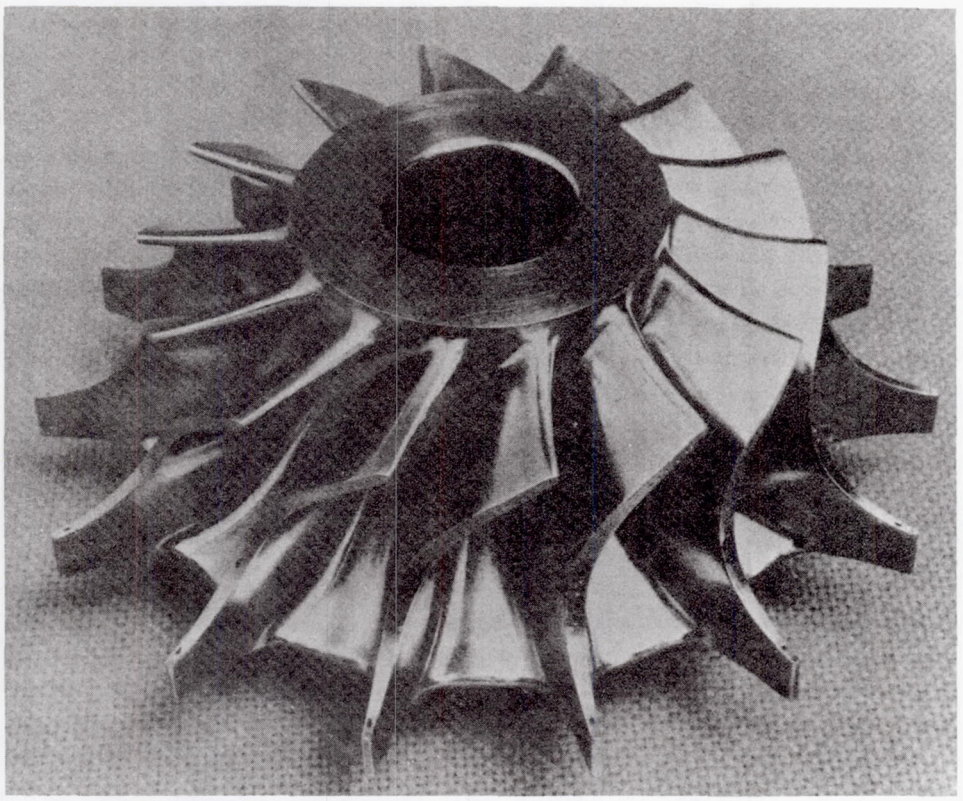

Figure 37. Finished laminated rotor.

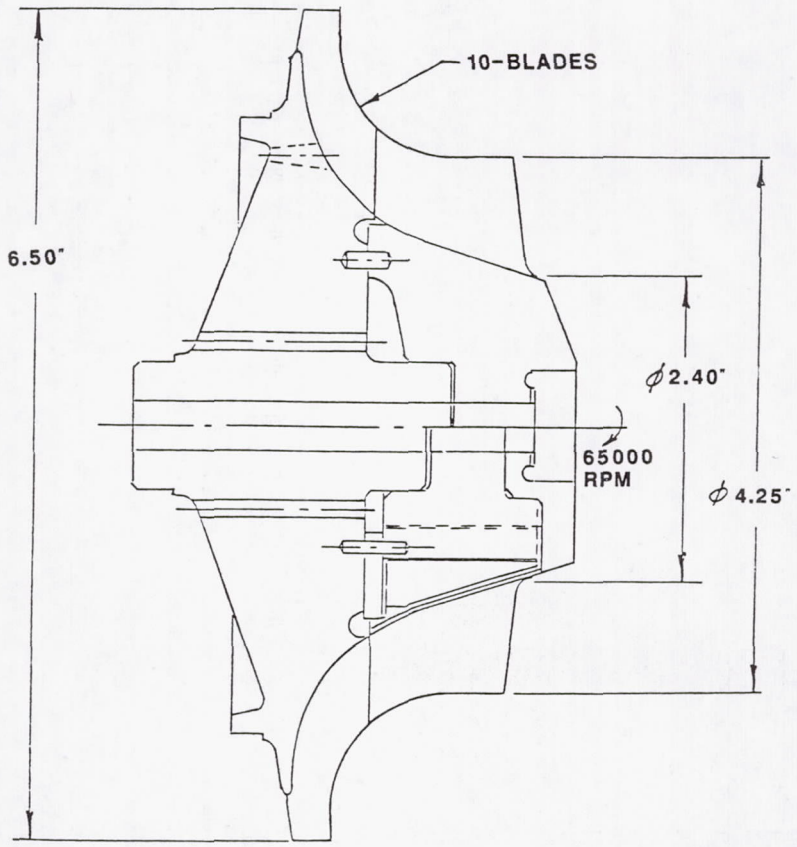

Figure 38. Cross section of split blade rotor.

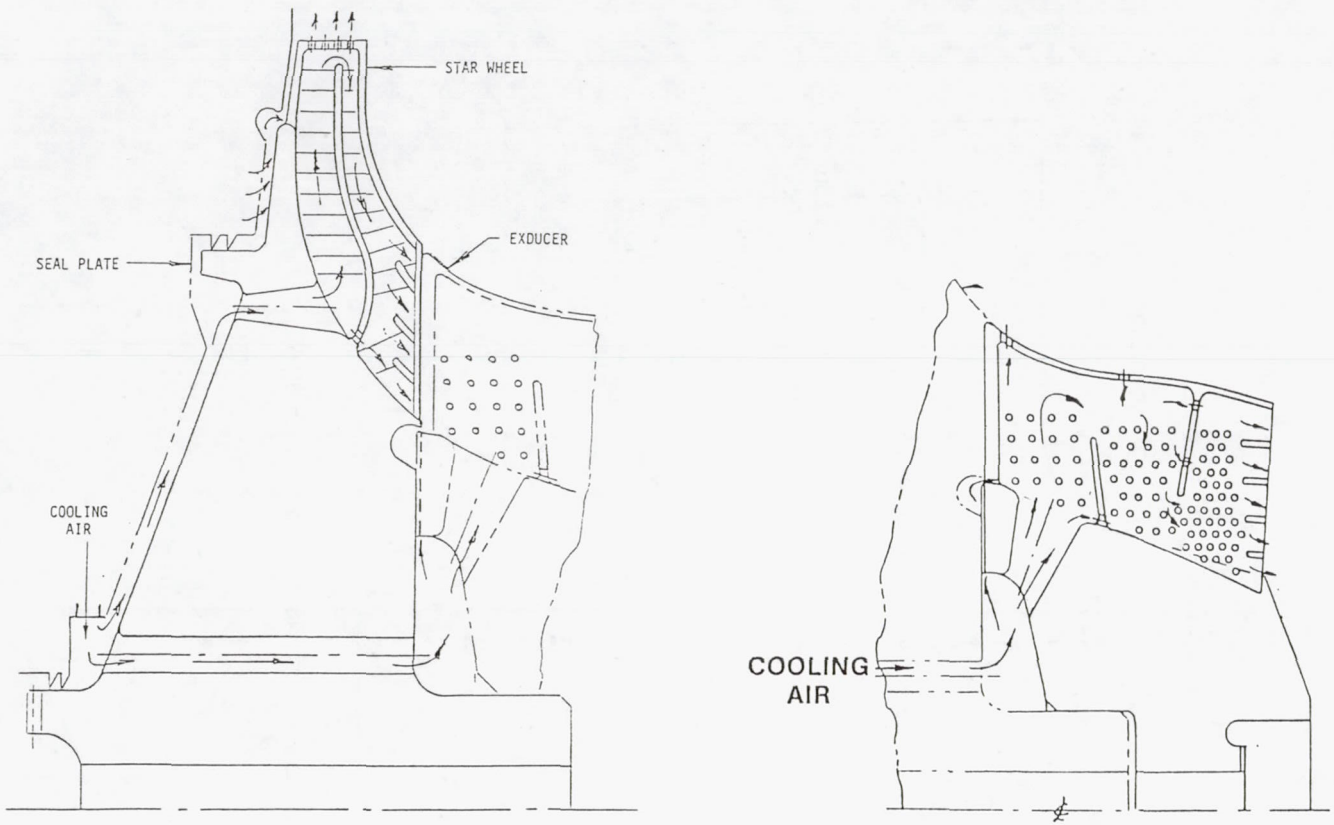

a) Star wheel

b) Exducer

Figure 39. Cooling geometry.

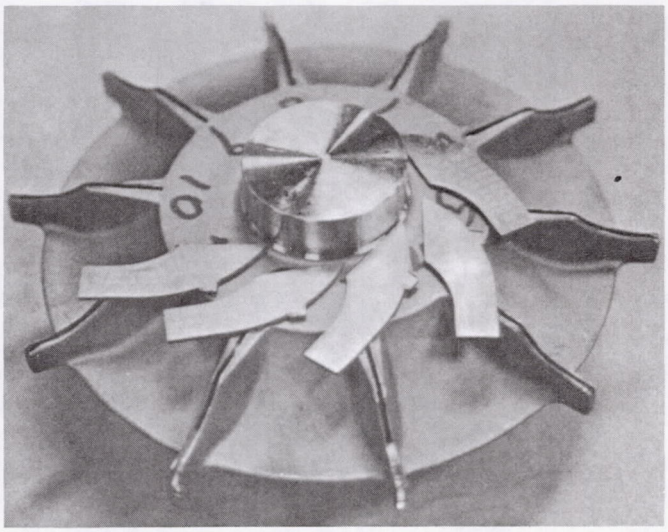

Figure 40. Machined star wheel and carrier assemblies.

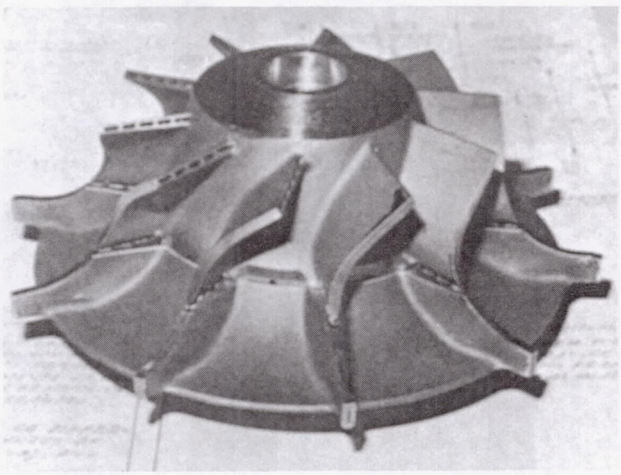

Figure 41. Completed split blade rotor.

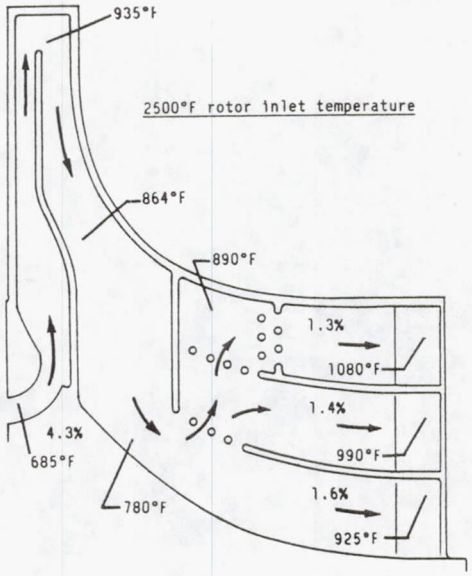

Figure 42. Cooling configuration of NASA research turbine.

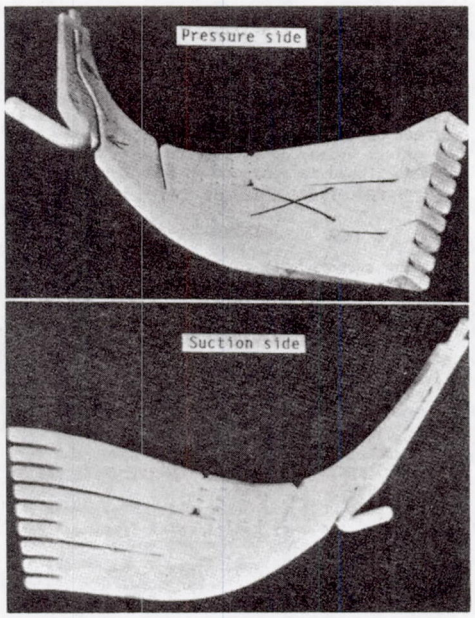

Figure 43. Ceramic cores for forming coolant passages.

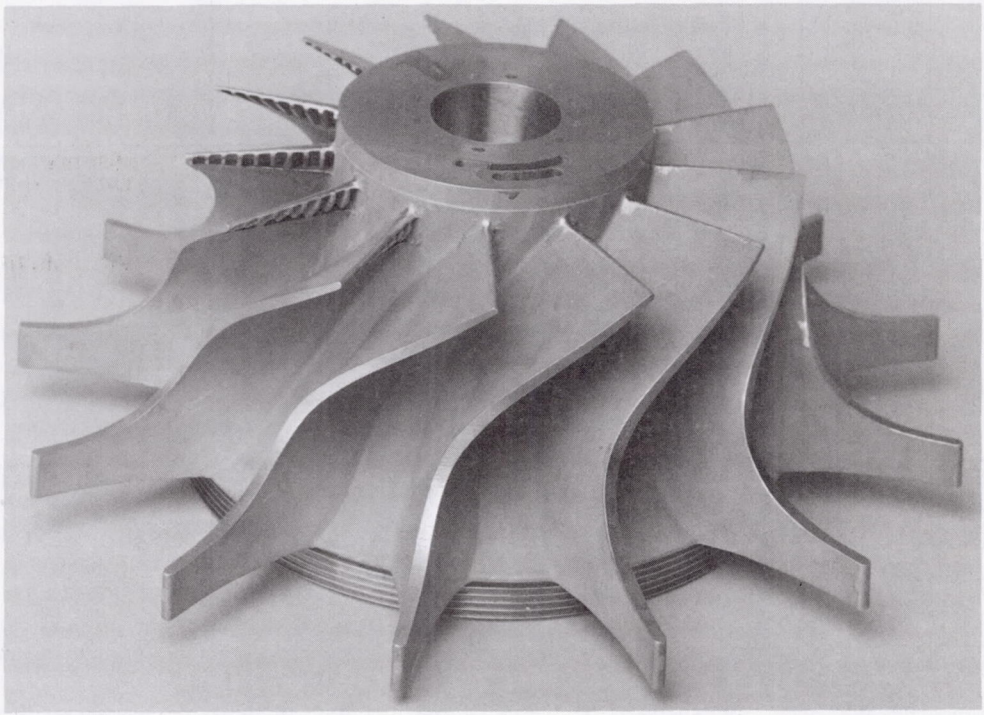

Figure 44. Cooled NASA research rotor.

REPORT DOCUMENTATION PAGE

Form Approved
OMB No. 0704-0188

1. AGENCY USE ONLY (*Leave blank*)	2. REPORT DATE	3. REPORT TYPE AND DATES COVERED
	April 1992	Technical Memorandum

4. TITLE AND SUBTITLE

Radial Turbine Cooling

5. FUNDING NUMBERS

WU–535–05–10

6. AUTHOR(S)

Richard J. Roelke

7. PERFORMING ORGANIZATION NAME(S) AND ADDRESS(ES)

National Aeronautics and Space Administration
Lewis Research Center
Cleveland, Ohio 44135–3191

8. PERFORMING ORGANIZATION REPORT NUMBER

E–7022

9. SPONSORING/MONITORING AGENCY NAMES(S) AND ADDRESS(ES)

National Aeronautics and Space Administration
Washington, D.C. 20546–0001

10. SPONSORING/MONITORING AGENCY REPORT NUMBER

NASA TM–105658

11. SUPPLEMENTARY NOTES

Presented at the Lecture Series on "Radial Turbines" at the von Karman Institute for Fluid Dynamics, Brussels, Belgium, April 6–10, 1992. Responsible person, Richard J. Roelke, (216) 433–3403.

12a. DISTRIBUTION/AVAILABILITY STATEMENT

Unclassified - Unlimited
Subject Category 02

12b. DISTRIBUTION CODE

13. ABSTRACT (*Maximum 200 words*)

Radial turbines have been used extensively in many applications including small ground based electrical power generators, automotive engine turbochargers and aircraft auxiliary power units. In all of these applications the turbine inlet temperature is limited to a value commensurate with the material strength limitations and life requirements of uncooled metal rotors. To take advantage that higher temperatures offer, such as increased turbine specific power output or higher cycle thermal efficiency, requires improved high temperature materials and/or blade cooling. Extensive research is on-going to advance the material properties of high temperature superalloys as well as composite materials including ceramics. The use of ceramics with their high temperature potential and low cost is particularly appealing for radial turbines. However until these programs reach fruition the only way to make significant step increases beyond the present material temperature barriers is to cool the radial blading.

14. SUBJECT TERMS	15. NUMBER OF PAGES
Turbines; Radial flow; Cooling	44
	16. PRICE CODE: A03

17. SECURITY CLASSIFICATION OF REPORT	18. SECURITY CLASSIFICATION OF THIS PAGE	19. SECURITY CLASSIFICATION OF ABSTRACT	20. LIMITATION OF ABSTRACT
Unclassified	Unclassified	Unclassified	

National Aeronautics and
Space Administration

Lewis Research Center
Cleveland, Ohio 44135

FOURTH CLASS MAIL

ADDRESS CORRECTION REQUESTED

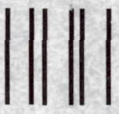

Official Business
Penalty for Private Use $300

Postage and Fees Paid
National Aeronautics and
Space Administration
NASA 451